

CONVERGENCE OF ADAPTIVE FEM FOR SOME ELLIPTIC OBSTACLE PROBLEM WITH INHOMOGENEOUS DIRICHLET DATA

MICHAEL FEISCHL, MARCUS PAGE, AND DIRK PRAETORIUS

Abstract. In this work, we show the convergence of adaptive lowest-order FEM (AFEM) for an elliptic obstacle problem with non-homogeneous Dirichlet data, where the obstacle χ is restricted only by $\chi \in H^2(\Omega)$. The adaptive loop is steered by some residual based error estimator introduced in BRAESS, CARSTENSEN & HOPPE (2007) that is extended to control oscillations of the Dirichlet data, as well. In the spirit of CASCON ET AL. (2008), we show that a weighted sum of energy error, estimator, and Dirichlet oscillations satisfies a contraction property up to certain vanishing energy contributions. This result extends the analysis of BRAESS, CARSTENSEN & HOPPE (2007) and PAGE & PRAETORIUS (2013) to the case of non-homogeneous Dirichlet data as well as certain non-affine obstacles and introduces some energy estimates to overcome the lack of nestedness of the discrete spaces.

Key words. Adaptive finite element methods, Elliptic obstacle problems, Convergence analysis.

1. Introduction

1.1. Comments on prior work. Adaptive finite element methods based on various types of a posteriori error estimators are a famous tool in science and engineering and are used to deal with a wide range of problems. As far as elliptic boundary value problems are concerned, convergence and even quasi-optimality of the adaptive scheme is well understood and analyzed, see e.g. [5, 16, 19, 29, 30, 37, 38].

In recent years the analysis has been extended and adapted to cover more general applications, such as the p -Laplacian [40], mixed methods [13], non-conforming elements [14], and obstacle problems. The latter is a classic introductory example to study variational inequalities which represent a whole class of problems that often arise in physical and economical context. One major application is the oscillation of a membrane that must stay above a certain obstacle. Other examples are filtration in porous media or the Stefan problem (i.e. melting solids), in both of which non-homogeneous Dirichlet data play an important role. Also in the financial world, obstacle problems arise, e.g. in the valuation of the American put option [34], where one has to deal with various non-affine obstacles. For a broader understanding of these problems, we refer to [21] and the references therein. The great applicability in many scientific areas thus make numerical analysis and mathematical understanding of the obstacle problem both, interesting and important. As far as a posteriori error analysis is concerned, we refer to [6, 8, 9, 17, 26, 31, 39]. Convergence of an adaptive method for elliptic obstacle problems with globally affine obstacle was proven in [10, 33]. Both of these works, however, considered homogeneous Dirichlet boundary data and affine obstacles only.

Received by the editors June 12, 2013.

2000 *Mathematics Subject Classification.* 65N30, 65N50.

In [11], the authors generalized the analysis of [10] to general $H^1(\Omega)$ -obstacles. Convergence of the proposed method is, however, only proved up to some consistency errors, and the analysis relies on homogeneous Dirichlet conditions. Moreover, some steps in the analysis are somewhat unclear, as the reliability proof depends on certain estimates which are not explained or properly cited.

1.2. Contributions of current work. We treat the case of a general obstacle $\chi \in H^2(\Omega)$. By a simple transformation and allowing non-homogeneous Dirichlet data (Prop. 4), this can, however, be reduced to the case of a constant zero-obstacle. Since our analysis works for general globally affine obstacles, even without the reduction step, we consider affine obstacles and non-homogeneous Dirichlet data in the following. We follow the ideas from [33], i.e. adaptive P1-FEM for some elliptic obstacle problem with globally affine obstacle. Contrary to [10, 11, 33], however, we allow non-homogeneous Dirichlet boundary data $g \in H^1(\Gamma)$, which are approximated by some g_ℓ via nodal interpolation within each step of the adaptive loop. In contrast to the aforementioned works, we thus do not have nestedness of the discrete ansatz sets, which is a crucial ingredient of the prior convergence proofs. In the spirit of [16] and in analogy to [33], we show that our adaptive algorithm, steered by some estimator ϱ_ℓ , guarantees that the combined error quantity

$$(1) \quad \Delta_\ell := \mathcal{J}(U_\ell) - \mathcal{J}(u_\ell) + \gamma \varrho_\ell^2 + \lambda \text{apx}_\ell^2$$

is a contraction up to some vanishing perturbations $\alpha_\ell \rightarrow 0$, i.e.

$$(2) \quad \Delta_{\ell+1} \leq \kappa \Delta_\ell + \alpha_\ell,$$

with $0 < \gamma, \kappa < 1, \lambda > 0$, and $\alpha_\ell \geq 0$. The data oscillations on the Dirichlet boundary are controlled by the term apx_ℓ , and the quantity u_ℓ denotes the continuous solution subject to discrete boundary data g_ℓ , which is introduced to circumvent the lack of nestedness of the discrete spaces. Convergence then follows from a weak reliability estimate of ϱ_ℓ , namely

$$(3) \quad \varrho_\ell \rightarrow 0 \quad \Rightarrow \quad \|u - U_\ell\|_{H^1(\Omega)} \rightarrow 0,$$

since $\varrho_\ell \lesssim \Delta_\ell \rightarrow 0$ as $\ell \rightarrow \infty$. We point out that our convergence proof makes use of the so called *estimator reduction* and is thus fairly independent of the mesh-refinement strategy. This is an improvement over the earlier works [10, 11] which rely on the *discrete local efficiency* of the underlying estimator and therefore require mesh-refinement strategies which guarantee the so-called *interior node property*.

1.3. Outline of current work. In Section 2, we formulate the continuous model problem and recall its unique solvability. In Section 3, the same is done for the discretized problem. Section 4 is a collection of the main results of this paper. Here, we introduce the error estimator ϱ_ℓ , which is a generalization of the corresponding estimators from [10, 33]. We then state its weak reliability (Theorem 7) and our version of the adaptive algorithm (Algorithm 9). Finally (Theorem 10), we state that the sequence of discrete solutions indeed converges towards the continuous solution $u \in H^1(\Omega)$. The subsequent Sections 5–7 are then devoted to the proofs of the aforementioned results and numerical illustrations.

2. Model Problem

2.1. Problem formulation. We consider an elliptic obstacle problem in \mathbb{R}^2 on a bounded Lipschitz domain Ω with polygonal boundary $\Gamma := \partial\Omega$. An obstacle

on $\overline{\Omega}$ is defined by the smooth function $\chi \in H^2(\Omega)$. Moreover, we consider inhomogeneous Dirichlet data $g \in H^{1/2}(\Gamma)$ and thus additionally require $\chi \leq g$ almost everywhere on Γ . As is usually done in practice, to define a local error estimator, we assume additional regularity $g \in H^1(\Gamma)$ in Section 4.2. By

$$(4) \quad \mathcal{A} := \{v \in H^1(\Omega) : v \geq \chi \text{ a.e. in } \Omega, v|_{\Gamma} = g \text{ a.e. on } \Gamma\},$$

we denote the set of admissible functions. For given $f \in L^2(\Omega)$, we consider the energy functional

$$(5) \quad \mathcal{J}(v) = \frac{1}{2} \langle v, v \rangle - (f, v),$$

with the bilinear form

$$(6) \quad \langle u, v \rangle = \int_{\Omega} \nabla u \cdot \nabla v \, dx \quad \text{for all } u, v \in H^1(\Omega)$$

and with the L^2 -scalar product

$$(7) \quad (f, v) = \int_{\Omega} f v \, dx.$$

By $\|\cdot\|$, we denote the energy norm on $H_0^1(\Omega)$ induced by $\langle \cdot, \cdot \rangle$. The obstacle problem then reads as follows: *Find $u \in \mathcal{A}$ such that*

$$(8) \quad \mathcal{J}(u) = \min_{v \in \mathcal{A}} \mathcal{J}(v).$$

2.2. Unique solvability. For the sake of completeness and to collect the main arguments needed below, we recall the proof that the obstacle problem (8) admits a unique solution. We stress that the following argument holds for any measurable obstacle χ with meaningful trace $\chi|_{\Gamma}$. Our restriction to smooth obstacles $\chi \in H^2(\Omega)$ is needed only for the equivalent reformulation in Section 2.3.

Proposition 1. *For given data $(\chi, g, f) \in H^2(\Omega) \times H^{1/2}(\Gamma) \times L^2(\Omega)$, the obstacle problem (8) admits a unique solution $u \in \mathcal{A}$ which is equivalently characterized by the variational inequality*

$$(9) \quad \langle u, v - u \rangle \geq (f, v - u)$$

for all $v \in \mathcal{A}$. □

The following two lemmata provide the essential ingredients to prove Proposition 1. We start with a well-known abstract result, cf. e.g. [7, Section 2.4–2.6].

Lemma 2. *Let \mathcal{H} be a Hilbert space with scalar product $\langle \cdot, \cdot \rangle$ and $\mathcal{K} \subseteq \mathcal{H}$ be a closed, convex, and non-empty subset. Then, for given $L \in \mathcal{H}^*$, the variational problem*

$$(10) \quad \mathcal{J}(u) = \min_{v \in \mathcal{K}} \mathcal{J}(v) \quad \text{with} \quad \mathcal{J}(v) = \frac{1}{2} \langle v, v \rangle - \langle L, v \rangle$$

has a unique solution $u \in \mathcal{K}$, where $\langle \cdot, \cdot \rangle$ denotes the dual pairing between \mathcal{H} and \mathcal{H}^* . In addition, this solution is equivalently characterized by the variational inequality

$$(11) \quad \langle u, v - u \rangle \geq \langle L, v - u \rangle$$

for all $v \in \mathcal{K}$. □

To apply Lemma 2, we observe that the obstacle problem (8) can be shifted into a setting with homogeneous Dirichlet data and $\mathcal{H} = H_0^1(\Omega)$. This involves a standard lifting operator $\mathcal{L} : H^{1/2}(\Gamma) \rightarrow H^1(\Omega)$, see e.g. [27, Theorem 3.37], with the properties

$$(12) \quad (\mathcal{L}v)|_\Gamma = v \quad \text{and} \quad \|\mathcal{L}v\|_{H^1(\Omega)} \leq C_1 \|v\|_{H^{1/2}(\Gamma)} \quad \text{for all } v \in H^{1/2}(\Gamma),$$

where the constant $C_1 > 0$ depends only on Ω .

With elementary algebraic manipulations, see e.g. [25, Section II.6], one obtains the following well-known link between the obstacle problem (8) and the abstract minimization problem (10) from Lemma 2.

Lemma 3. *Let $\widehat{g} \in H^1(\Omega)$ be an arbitrary extension of $g \in H^{1/2}(\Gamma)$, e.g., $\widehat{g} = \mathcal{L}g$. For $u \in \mathcal{A}$ and $u - \widehat{g} = \tilde{u} \in \mathcal{K} := \{\tilde{v} \in H_0^1(\Omega) : \tilde{v} \geq \chi - \widehat{g}\}$, the following statements are equivalent:*

- (i) u solves the obstacle problem (8).
- (ii) u satisfies $\langle u, v - u \rangle \geq \langle f, v - u \rangle$ for all $v \in \mathcal{A}$.
- (iii) \tilde{u} satisfies $\langle \tilde{u}, \tilde{v} - \tilde{u} \rangle \geq \langle f, \tilde{v} - \tilde{u} \rangle - \langle \widehat{g}, \tilde{v} - \tilde{u} \rangle$ for all $\tilde{v} \in \mathcal{K}$. □

We thus conclude that the continuous obstacle problem

$$(13a) \quad \mathcal{J}(u) = \min_{v \in \mathcal{A}} \mathcal{J}(v),$$

with the set of admissible functions

$$(13b) \quad \mathcal{A} := \{v \in H^1(\Omega) : v \geq \chi \text{ a.e. in } \Omega, v|_\Gamma = g \text{ a.e. on } \Gamma\},$$

admits a unique solution. Moreover, standard arguments show that this solution does not depend on the special choice of \widehat{g} .

2.3. Reduction to problem with zero obstacle. The following proposition allows us to restrict the considered problem (13) with $H^2(\Omega)$ -obstacle to the case where the obstacle χ is even zero. This provides the formulation which can be treated by our adaptive method below.

Proposition 4. *For some smooth obstacle $\chi \in H^2(\Omega)$, the obstacle problem (13) with data (χ, g, f) is equivalent to the obstacle problem with data $(0, g - \chi|_\Gamma, f + \Delta\chi)$. If $\tilde{u} \in H^1(\Omega)$ solves the obstacle problem with data $(0, g - \chi|_\Gamma, f + \Delta\chi)$, $u = \tilde{u} + \chi$ is the unique solution with respect to the data (χ, g, f) .*

Proof. The solution $u \in \mathcal{A}$ of the obstacle problem with data (χ, g, f) is characterized by

$$\langle u, v - u \rangle \geq \langle f, v - u \rangle$$

for all $v \in \mathcal{A} = \{v \in H^1(\Omega) : v \geq \chi \text{ a.e. in } \Omega, v|_\Gamma = g\}$. Substitution $\tilde{u} := u - \chi$ and $\tilde{v} := v - \chi$ shows that this is equivalent to

$$\langle \tilde{u}, \tilde{v} - \tilde{u} \rangle \geq \langle f, \tilde{v} - \tilde{u} \rangle - \langle \chi, \tilde{v} - \tilde{u} \rangle \quad \text{for all } \tilde{v} \in \tilde{\mathcal{A}},$$

where $\tilde{\mathcal{A}} := \{\tilde{v} \in H^1(\Omega) : \tilde{v} \geq 0 \text{ a.e. in } \Omega, \tilde{v}|_\Gamma = g - \chi|_\Gamma\}$. Finally, integration by parts with $w := \tilde{v} - \tilde{u} \in H_0^1(\Omega)$ proves

$$-\langle \chi, \tilde{v} - \tilde{u} \rangle = - \int_\Omega \nabla \chi \cdot \nabla w \, dx = \int_\Omega \Delta \chi w \, dx.$$

This concludes the proof. □

2.4. Model problem. According to the observation of Proposition 4, we may restrict to the case $\chi = 0$ in the following. Having obtained a FE approximation U_ℓ of u for the zero obstacle case, we may simply consider $\tilde{U}_\ell := U_\ell + \chi$ to obtain an approximation of the original problem with obstacle $\chi \in H^2(\Omega)$. Note that the overall error is then equivalent to the error of the reduced obstacle problem since

$$\|u - U_\ell\|_{H^1(\Omega)} = \|u - \chi - U_\ell + \chi\|_{H^1(\Omega)} = \|\tilde{u} - \tilde{U}_\ell\|_{H^1(\Omega)}.$$

Since our analysis directly covers affine obstacles, we shall, however, allow that χ is globally affine rather than simply zero on $\bar{\Omega}$. Put explicitly, we consider Problem (13) with respect to the data $(\chi, g, f) \in \mathcal{P}^1(\bar{\Omega}) \times H^1(\Gamma) \times L^2(\Omega)$, i.e. we may avoid the reformulation of Proposition 4 in this particular case. As mentioned above, we again emphasize the assumed additional regularity $g \in H^1(\Gamma)$.

3. Galerkin Discretization

3.1. Problem formulation. For the numerical solution of (13) by means of an adaptive finite element method, we consider conforming and in the sense of Ciarlet regular triangulations \mathcal{T}_ℓ of Ω and denote the standard P1-FEM space of globally continuous and piecewise affine functions by $\mathcal{S}^1(\mathcal{T}_\ell)$. Note that a discrete function $V_\ell \in \mathcal{S}^1(\mathcal{T}_\ell)$ cannot satisfy the inhomogeneous Dirichlet conditions g in general. We therefore have to approximate $g \approx g_\ell \in \mathcal{S}^1(\mathcal{T}_\ell|_\Gamma)$, where the space $\mathcal{S}^1(\mathcal{T}_\ell|_\Gamma) := \{V_\ell|_\Gamma : V_\ell \in \mathcal{S}^1(\mathcal{T}_\ell)\}$ denotes the space of globally continuous and piecewise affine functions on the boundary Γ . For this discretization, we assume additional regularity $g \in H^1(\Gamma)$ and consider the approximation $g_\ell \in \mathcal{S}^1(\mathcal{T}_\ell|_\Gamma)$ which is derived by nodal interpolation of the boundary data. Note that nodal interpolation is well-defined since the Sobolev inequality on the 1D manifold Γ predicts the continuous inclusion $H^1(\Gamma) \subset C(\Gamma)$. Altogether, the set of discrete admissible functions \mathcal{A}_ℓ is given by

$$(14a) \quad \mathcal{A}_\ell := \{V_\ell \in \mathcal{S}^1(\mathcal{T}_\ell) : V_\ell \geq \chi \text{ in } \Omega, V_\ell = g_\ell \text{ on } \Gamma\},$$

and the discrete minimization problem reads: Find $U_\ell \in \mathcal{A}_\ell$ such that

$$(14b) \quad \mathcal{J}(U_\ell) = \min_{V_\ell \in \mathcal{A}_\ell} \mathcal{J}(V_\ell).$$

Remark 5. Note that $\chi \leq g \in H^1(\Gamma) \subset C(\Gamma)$, implies that $\chi(z) \leq g(z) = g_\ell(z)$ for all nodes $z \in \Gamma$. Since χ is affine, we conclude $\chi \leq g_\ell$ on Γ for the nodal interpolant $g_\ell \in \mathcal{S}^1(\mathcal{T}_\ell|_\Gamma)$.

3.2. Notation. From now on, \mathcal{N}_ℓ denotes the set of nodes of the regular triangulation \mathcal{T}_ℓ . The set of all interior edges $E = T^+ \cap T^-$ for certain elements $T^+, T^- \in \mathcal{T}_\ell$ is denoted by \mathcal{E}_ℓ^Ω . The set of all edges of \mathcal{T}_ℓ is denoted by \mathcal{E}_ℓ . In particular, $\mathcal{E}_\ell|_\Gamma := \mathcal{E}_\ell^\Gamma := \mathcal{E}_\ell \setminus \mathcal{E}_\ell^\Omega$ contains all boundary edges and provides some partition of Γ .

We recall that $\mathcal{S}^1(\mathcal{T}_\ell) = \{V_\ell \in C(\bar{\Omega}) : V_\ell|_T \text{ affine for all } T \in \mathcal{T}_\ell\}$ denotes the conforming P1-finite element space. Moreover, $\mathcal{S}_0^1(\mathcal{T}_\ell) = \mathcal{S}^1(\mathcal{T}_\ell) \cap H_0^1(\Omega) = \{V_\ell \in \mathcal{S}^1(\mathcal{T}_\ell) : V_\ell|_\Gamma = 0\}$.

3.3. Unique solvability. In this section, we recall that the discrete obstacle problem (14) admits a unique solution which is again characterized by a variational inequality.

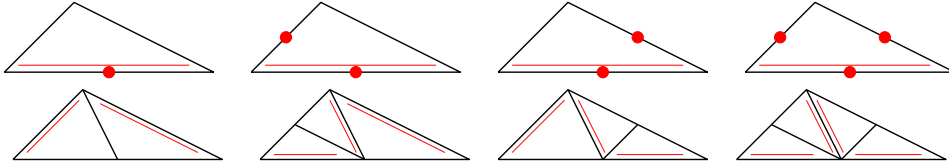


FIGURE 1. For each triangle $T \in \mathcal{T}$, there is one fixed *reference edge*, indicated by the double line (left, top). Refinement of T is done by bisecting the reference edge, where its midpoint becomes a new node. The reference edges of the son triangles are opposite to this newest vertex (left, bottom). To avoid hanging nodes, one proceeds as follows: We assume that certain edges of T , but at least the reference edge, are marked for refinement (top). Using iterated newest vertex bisection, the element is then split into 2, 3, or 4 son triangles (bottom).

Proposition 6. *The discrete obstacle problem (14) admits a unique solution $U_\ell \in \mathcal{A}_\ell$, which is equivalently characterized by the variational inequality*

$$(15) \quad \langle U_\ell, V_\ell - U_\ell \rangle \geq \langle f, V_\ell - U_\ell \rangle$$

for all $V_\ell \in \mathcal{A}_\ell$. □

The proof of Proposition 6 is obtained as in the continuous case. It relies on the fact that discrete boundary data $g_\ell \in \mathcal{S}^1(\mathcal{T}_\ell|_\Gamma)$ can be lifted to a discrete function $\hat{g}_\ell \in \mathcal{S}^1(\mathcal{T}_\ell)$ with $\hat{g}_\ell|_\Gamma = g_\ell$. The proof of the latter is a consequence of (and even equivalent to, see [18]) the existence of the Scott-Zhang quasi-interpolation operator $P_\ell : H^1(\Omega) \rightarrow \mathcal{S}^1(\mathcal{T}_\ell)$, see [36], which is a linear and continuous projection onto $\mathcal{S}^1(\mathcal{T}_\ell)$, i.e.

$$(16) \quad P_\ell^2 = P_\ell \quad \text{and} \quad \|P_\ell v\|_{H^1(\Omega)} \leq C_2 \|v\|_{H^1(\Omega)}, \quad \text{for all } v \in H^1(\Omega),$$

that preserves discrete boundary conditions, i.e.

$$(17) \quad (P_\ell v)|_\Gamma = v|_\Gamma \quad \text{for all } v \in H^1(\Omega) \text{ with } v|_\Gamma \in \mathcal{S}^1(\mathcal{T}_\ell|_\Gamma).$$

The constant $C_2 > 0$ depends only on the shape regularity constant $\sigma(\mathcal{T}_\ell)$ and on the diameter of Ω . Moreover, P_ℓ has a local first-order approximation property which is, however, not used throughout.

4. Adaptive Mesh-Refining Algorithm and Main Results

4.1. Newest vertex bisection. For the mesh-refinement, we use newest-vertex bisection. Assume that $\mathcal{M}_\ell \subseteq \mathcal{E}_\ell$ is a set of edges which have to be refined. The refinement rules are shown in Figure 1, and the reader is also referred to [38, Chapter 5]. We stress a certain decay of the mesh-widths:

- Marked edges $E \in \mathcal{M}_\ell$ are split into two edges $E', E'' \in \mathcal{E}_{\ell+1}$ of half length, i.e. new nodes $z \in \mathcal{N}_{\ell+1} \setminus \mathcal{N}_\ell$ are always midpoints of refined edges $E \in \mathcal{E}_\ell \setminus \mathcal{E}_{\ell+1}$.
- If at least one edge E of an element $T \in \mathcal{T}_\ell$ is marked, T is refined into up to four son elements $T' \in \mathcal{T}_{\ell+1}$ with area $|T|/4 \leq |T'| \leq |T|/2$, cf. Figure 1.

Moreover, given an initial mesh \mathcal{T}_0 , newest vertex bisection only leads to at most $4 \cdot \#\mathcal{T}_0$ similarity classes of triangles. In particular, the generated meshes are

uniformly shape regular

$$(18) \quad \sup_{\ell \in \mathbb{N}} \sigma(\mathcal{T}_\ell) < \infty \quad \text{with} \quad \sigma(\mathcal{T}_\ell) = \max_{T \in \mathcal{T}_\ell} \frac{\text{diam}(T)^2}{|T|}.$$

Furthermore, the number of different shapes of e.g. node patches that can occur, is finite. These observations will be necessary in the scaling arguments below.

4.2. Weakly reliable error estimator. Let $u \in \mathcal{A}$ denote the continuous solution of (13) and $U_\ell \in \mathcal{A}_\ell$ be the discrete solution of (14) for some fixed triangulation \mathcal{T}_ℓ . To steer the adaptive mesh-refinement, we use some residual-based error estimator

$$(19) \quad \varrho_\ell^2 := \sum_{E \in \mathcal{E}_\ell^\Omega} (\eta_\ell(E)^2 + \text{osc}_\ell(E)^2) + \sum_{E \in \mathcal{E}_\ell^\Gamma} (\text{apx}_\ell(E)^2 + \text{osc}_\ell(E)^2)$$

which has essentially been introduced in [10] for homogeneous Dirichlet data $g = 0$. First, $\eta_\ell(E)^2$ denotes the weighted L^2 -norms of the normal jump

$$(20) \quad \eta_\ell(E)^2 := h_E \|\llbracket \partial_n U_\ell \rrbracket\|_{L^2(E)}^2 \quad \text{for } E \in \mathcal{E}_\ell^\Omega$$

with $h_E = \text{diam}(E)$ the length of E and $\llbracket \cdot \rrbracket$ the jump over an interior edge $E = T^+ \cap T^- \in \mathcal{E}_\ell^\Omega$. Second, for interior edges, $\text{osc}_\ell(E)^2$ denotes the data oscillations of f

$$(21) \quad \text{osc}_\ell(E)^2 := |\Omega_{\ell,E}| \|f - f_{\Omega_{\ell,E}}\|_{L^2(\Omega_{\ell,E})}^2 \quad \text{for } E \in \mathcal{E}_\ell^\Omega$$

over the patch $\Omega_{\ell,E} = T^+ \cup T^-$ associated with E , where the corresponding integral mean of f is denoted by $f_{\Omega_{\ell,E}} = (1/|\Omega_{\ell,E}|) \int_{\Omega_{\ell,E}} f \, dx$. Third, for boundary edges $E \in \mathcal{E}_\ell^\Gamma$ and $T \in \mathcal{T}_\ell$ the unique element with $E \subseteq \partial T \cap \Gamma$, ϱ_ℓ involves the weighted element residuals

$$(22) \quad \text{osc}_\ell(E)^2 := |T| \|f\|_{L^2(T)}^2 \quad \text{for } E \in \mathcal{E}_\ell^\Gamma.$$

Finally and in order to control the approximation of the nonhomogeneous Dirichlet data g by its nodal interpolant g_ℓ , we apply an idea from [4] and use

$$(23) \quad \text{apx}_\ell(E)^2 := h_E \|(g - g_\ell)'\|_{L^2(E)}^2 \quad \text{for } E \in \mathcal{E}_\ell^\Gamma,$$

where $(\cdot)'$ denotes the arclength derivative. Here, we exploit the additional regularity assumption $g \in H^1(\Gamma)$, see Section 2.4.

To state a reliability result for the proposed error estimator ϱ_ℓ , we need to introduce a continuous auxiliary problem, which considers the continuous case subject to the discretized boundary data. Given the discrete Dirichlet data $g_\ell \in \mathcal{S}^1(\mathcal{T}_\ell|_\Gamma)$, we define

$$(24a) \quad \mathcal{A}_\ell^* := \{v_\ell \in H^1(\Omega) : v_\ell \geq \chi \text{ a.e. in } \Omega, v_\ell|_\Gamma = g_\ell \text{ a.e. on } \Gamma\}.$$

Applying Proposition 1 for the data (χ, g_ℓ, f) , we see that the auxiliary problem

$$(24b) \quad \mathcal{J}(u_\ell) = \min_{v_\ell \in \mathcal{A}_\ell^*} \mathcal{J}(v_\ell)$$

admits a unique solution $u_\ell \in \mathcal{A}_\ell^*$. The following theorem now states weak reliability of ϱ_ℓ in the sense that $\varrho_\ell \rightarrow 0$ implies $\|u - U_\ell\|_{H^1(\Omega)} \rightarrow 0$ as $\ell \rightarrow \infty$. The proof is given in Section 5 below.

Theorem 7. *With $u_\ell \in \mathcal{A}_\ell^*$ the solution of the auxiliary problem (24), the error estimator ϱ_ℓ from (19) satisfies*

$$(25) \quad \frac{1}{2} \|u_\ell - U_\ell\|^2 \leq \mathcal{J}(U_\ell) - \mathcal{J}(u_\ell) \leq C_3^2 \tilde{\varrho}_\ell^2,$$

with

$$(26) \quad \tilde{\varrho}_\ell^2 := \sum_{E \in \mathcal{E}_\ell^\Omega} (\eta_\ell(E)^2 + \text{osc}_\ell(E)^2) + \sum_{E \in \mathcal{E}_\ell^\Gamma} \text{osc}_\ell(E)^2,$$

as well as

$$(27) \quad \|u - U_\ell\|_{H^1(\Omega)} \leq \|u - u_\ell\| + \sqrt{2}C_3 \varrho_\ell,$$

where the constant $C_3 > 0$ depends only on $\sigma(\mathcal{T}_\ell)$ and on Ω . Moreover, there holds

$$(28) \quad \varrho_\ell \xrightarrow{\ell \rightarrow \infty} 0 \implies \|u - U_\ell\|_{H^1(\Omega)} \xrightarrow{\ell \rightarrow \infty} 0.$$

Remark 8. We stress that the reliability estimate (25) depends on χ being affine and the use of newest vertex bisection in the sense that only finitely many shapes of node patches and edge patches can occur. For red-green-blue refinement [38, Chapter 5], the equivalence of edge and node oscillations is open. The entire analysis, however, even applies for a coarser error estimator, where edge oscillations are bounded in terms of the element residuals $\|h_\ell f\|_{L^2(T)}$.

4.3. Convergent adaptive mesh-refining algorithm. We can now state our version of the adaptive algorithm in the usual form:

$$\boxed{\text{Solve}} \mapsto \boxed{\text{Estimate}} \mapsto \boxed{\text{Mark}} \mapsto \boxed{\text{Refine}}$$

Throughout, we assume that the Galerkin solution $U_\ell \in \mathcal{S}^1(\mathcal{T}_\ell)$ is computed exactly. For the marking step, we use the strategy proposed by Dörfler [19].

Algorithm 9. Fix an adaptivity parameter $0 < \theta < 1$, let \mathcal{T}_ℓ with $\ell = 0$ be the initial triangulation, and fix a reference edge for each element $T \in \mathcal{T}_0$. For each $\ell = 0, 1, 2, \dots$ do:

- (i) Compute discrete solution $U_\ell \in \mathcal{A}_\ell$.
 - (ii) Compute $\eta_\ell(E)^2$, $\text{osc}_\ell(E)^2$, and $\text{apx}_\ell(E)^2$ for all $E \in \mathcal{E}_\ell$.
 - (iii) Determine set $\mathcal{M}_\ell \subseteq \mathcal{E}_\ell$ of minimal cardinality, which satisfies
- $$(29) \quad \theta \varrho_\ell^2 \leq \sum_{E \in \mathcal{E}_\ell^\Omega \cap \mathcal{M}_\ell} (\eta_\ell(E)^2 + \text{osc}_\ell(E)^2) + \sum_{E \in \mathcal{E}_\ell^\Gamma \cap \mathcal{M}_\ell} (\text{apx}_\ell(E)^2 + \text{osc}_\ell(E)^2).$$

- (iv) Mark all edges $E \in \mathcal{M}_\ell$ for refinement and obtain new mesh $\mathcal{T}_{\ell+1}$ by newest vertex bisection.
- (v) Increase counter $\ell \mapsto \ell + 1$ and iterate. □

The following theorem states our main convergence results.

Theorem 10. Algorithm 9 guarantees the existence of constants $0 < \kappa, \gamma < 1$ and $\lambda > 0$ and a sequence $\alpha_\ell \geq 0$ with $\lim_{\ell \rightarrow \infty} \alpha_\ell = 0$ such that the combined error quantity

$$(30) \quad \Delta_\ell := \mathcal{J}(U_\ell) - \mathcal{J}(u_\ell) + \gamma \varrho_\ell^2 + \lambda \text{apx}_\ell^2 \geq 0$$

satisfies contraction up to the zero sequence α_ℓ , i.e.

$$(31) \quad \Delta_{\ell+1} \leq \kappa \Delta_\ell + \alpha_\ell \quad \text{for all } \ell \in \mathbb{N}.$$

In particular, this implies

$$(32) \quad 0 = \lim_{\ell \rightarrow \infty} \Delta_\ell = \lim_{\ell \rightarrow \infty} \varrho_\ell = \lim_{\ell \rightarrow \infty} \|u - U_\ell\|_{H^1(\Omega)}$$

as well as convergence of the energies

$$(33) \quad \mathcal{J}(u) = \lim_{\ell \rightarrow \infty} \mathcal{J}(u_\ell) = \lim_{\ell \rightarrow \infty} \mathcal{J}(U_\ell).$$

5. Proof of Theorem 7 (Weak Reliability of Error Estimator)

5.1. Stability of continuous problem. For the finite element discretization, we have to replace the continuous Dirichlet data $g \in H^{1/2}(\Gamma)$ by appropriate discrete functions g_ℓ . To make this procedure feasible, we have to prove that the solution of the obstacle problem (13) depends continuously on the given data.

In the following, let \mathcal{H} be a Hilbert space with scalar product $\langle \cdot, \cdot \rangle$ and $\mathcal{K}, \mathcal{K}_\ell^* \subset \mathcal{H}$ be closed, convex, and non-empty subsets of \mathcal{H} . We say, that \mathcal{K}_ℓ^* converges to \mathcal{K} in the sense of Mosco [28] if and only if

$$(34) \quad \forall v \in \mathcal{K} \exists v_\ell \in \mathcal{K}_\ell^* : v_\ell \rightarrow v \text{ strongly in } \mathcal{H} \text{ as } \ell \rightarrow \infty$$

and

$$(35) \quad \forall v \in \mathcal{H} \forall v_\ell \in \mathcal{K}_\ell^* : (v_\ell \rightharpoonup v \text{ weakly in } \mathcal{H} \implies v \in \mathcal{K}).$$

Put explicitly, we say that the set \mathcal{K}_ℓ^* converges towards the set \mathcal{K} if every $v \in \mathcal{K}$ is the limit of a sequence $v_\ell \in \mathcal{K}_\ell^*$, and if the limit v of any converging sequence $v_\ell \in \mathcal{K}_\ell^*$ is automatically in \mathcal{K} . The set \mathcal{K} is thus somewhat the collection of all limits of the converging sequences from \mathcal{K}_ℓ^* . We can now state an abstract stability result of Mosco:

Lemma 11 ([28, Theorem A]). *Assume the sets $\mathcal{K}, \mathcal{K}_\ell^*$ satisfy (34)–(35). Let $L, L_\ell \in \mathcal{H}^*$ be functionals and assume $L_\ell \rightarrow L$ in \mathcal{H}^* as $\ell \rightarrow \infty$. Finally, let $u \in \mathcal{K}$ and $u_\ell \in \mathcal{K}_\ell^*$ be the unique solutions of (10) with respect to the data (\mathcal{K}, L) and $(\mathcal{K}_\ell^*, L_\ell)$, respectively. Then there holds strong convergence*

$$(36) \quad u_\ell \rightarrow u \text{ in } \mathcal{H} \text{ as } \ell \rightarrow \infty,$$

i.e. the solution of the variational problem (10) depends continuously on the given data. \square

Remark 12. *We remark that we have stated [28, Theorem A] only in a simplified form. In general, the preceding lemma of Mosco includes the approximation of the bilinear form $\langle \cdot, \cdot \rangle$ as well, and it also holds for nonlinear variational inequalities, where the underlying operators $A_\ell, A : \mathcal{H} \rightarrow \mathcal{H}^*$, e.g. $A v := \langle v, \cdot \rangle$, are assumed to be Lipschitz continuous and strictly monotone with constants independent of ℓ .*

We are now in the position to show that the solution $u \in \mathcal{A}$ of the obstacle problem (13) continuously depends on the boundary data $g \in H^{1/2}(\Gamma)$.

Proposition 13. *Recall that $u_\ell \in \mathcal{A}_\ell^*$ denotes the solution of the auxiliary problem (24). Provided convergence $g_\ell \rightarrow g$ in $H^{1/2}(\Gamma)$ of the Dirichlet data, there also holds convergence $u_\ell \rightarrow u$ in $H^1(\Omega)$ of the (continuous) solutions as $\ell \rightarrow \infty$.*

Proof. As in the proof of Proposition 1, we define the sets

$$\mathcal{K} = \{\tilde{v} \in H_0^1(\Omega) : \tilde{v} \geq \chi - \mathcal{L}g\} \quad \text{and} \quad \mathcal{K}_\ell^* = \{\tilde{v}_\ell \in H_0^1(\Omega) : \tilde{v}_\ell \geq \chi - \mathcal{L}g_\ell\}.$$

We stress that both sets are convex, closed, and non-empty subsets of $H_0^1(\Omega)$. As usual, let $H^{-1}(\Omega) := H_0^1(\Omega)^*$ denote the dual space of $H_0^1(\Omega)$. With respect to the abstract notation, we have $L, L_\ell \in H^{-1}(\Omega)$ with

$$\langle L, \tilde{v} \rangle = (f, \tilde{v}) - \langle \mathcal{L}g, \tilde{v} \rangle \quad \text{and} \quad \langle L_\ell, \tilde{v} \rangle = (f, \tilde{v}) - \langle \mathcal{L}g_\ell, \tilde{v} \rangle.$$

Note that this implies

$$\|L - L_\ell\|_{H^{-1}(\Omega)} \leq \|\mathcal{L}g - \mathcal{L}g_\ell\|_{H^1(\Omega)} \lesssim \|g - g_\ell\|_{H^{1/2}(\Gamma)} \xrightarrow{\ell \rightarrow \infty} 0.$$

Next, we prove that $\mathcal{K}_\ell^* \rightarrow \mathcal{K}$ in the sense of Mosco (34)–(35).

To verify (34), let $\tilde{v} \in \mathcal{K}$ be arbitrary. Define

$$v := \tilde{v} + \mathcal{L}g \in \mathcal{A}$$

and let $w_\ell \in H^1(\Omega)$ be the unique solution of the (linear) auxiliary problem

$$\Delta w_\ell = 0 \text{ in } \Omega \quad \text{with Dirichlet conditions} \quad w_\ell = g_\ell - g \text{ on } \Gamma.$$

In the next step, we consider

$$\bar{v}_\ell := v + w_\ell \in H^1(\Omega).$$

Then, there holds $\bar{v}_\ell|_\Gamma = g_\ell$ as well as

$$\|v - \bar{v}_\ell\|_{H^1(\Omega)} = \|w_\ell\|_{H^1(\Omega)} \lesssim \|g_\ell - g\|_{H^{1/2}(\Gamma)} \xrightarrow{\ell \rightarrow \infty} 0.$$

Since the maximum of H^1 -functions belongs to H^1 , we obtain

$$v_\ell := \max\{\chi, \bar{v}_\ell\} \in H^1(\Omega).$$

By definition, there holds $v_\ell \geq \chi$ almost everywhere in Ω as well as $v_\ell|_\Gamma = g_\ell$ since $\bar{v}_\ell|_\Gamma = g_\ell \geq \chi|_\Gamma$ almost everywhere on Γ , see Remark 5. Altogether, this proves $v_\ell \in \mathcal{A}_\ell$. Moreover, since the function $\max\{\chi, \cdot\} : H^1(\Omega) \rightarrow H^1(\Omega)$ is well-defined and continuous (see e.g. [22, Chapter II, Corollary 2.1]), there holds

$$v = \max\{\chi, v\} = \lim_{\ell \rightarrow \infty} \max\{\chi, \bar{v}_\ell\} = \lim_{\ell \rightarrow \infty} v_\ell \text{ in } H^1(\Omega).$$

Finally, we observe

$$\tilde{v}_\ell := v_\ell - \mathcal{L}g_\ell \xrightarrow{\ell \rightarrow \infty} v - \mathcal{L}g = \tilde{v} \text{ in } H^1(\Omega)$$

and $\tilde{v}_\ell \in \mathcal{K}_\ell^*$.

To verify (35), let $v_\ell \in \mathcal{K}_\ell^*$ and assume that the weak limit $v_\ell \rightharpoonup v \in H_0^1(\Omega)$ exists as $\ell \rightarrow \infty$. According to the Rellich compactness theorem, there is a subsequence (v_{ℓ_k}) which converges strongly to v in $L^2(\Omega)$. According to the Weyl theorem, we may thus extract a further subsequence $(v_{\ell_{k_j}})$ which converges to v pointwise almost everywhere in Ω . Moreover, by continuity of the lifting operator, there holds $\mathcal{L}g_{\ell_{k_j}} \rightarrow \mathcal{L}g$ in $H^1(\Omega)$ as $j \rightarrow \infty$. Since this implies L^2 -convergence and again according to the Weyl theorem, we may choose a subsequence $(\mathcal{L}g_{\ell_{k_{j_i}}})$ which converges to $\mathcal{L}g$ pointwise almost everywhere in Ω . Altogether, the estimate

$$v_{\ell_{k_{j_i}}} \geq \chi - \mathcal{L}g_{\ell_{k_{j_i}}} \quad \text{a.e. in } \Omega$$

and monotonicity of the pointwise limit imply

$$v \geq \chi - \mathcal{L}g \quad \text{a.e. in } \Omega,$$

whence $v \in \mathcal{K}$.

Now, we may apply Lemma 11 to see that the unique solutions $\tilde{u} \in \mathcal{K}$ and $\tilde{u}_\ell \in \mathcal{K}_\ell^*$ of the minimization problems (10) with respect to the data (\mathcal{K}, L) and $(\mathcal{K}_\ell^*, L_\ell)$, respectively, guarantee

$$\|\tilde{u} - \tilde{u}_\ell\|_{H^1(\Omega)} \xrightarrow{\ell \rightarrow \infty} 0.$$

With Lemma 3, there holds $u = \tilde{u} + \mathcal{L}g$ as well as $u_\ell = \tilde{u}_\ell + \mathcal{L}g_\ell$. Altogether, we thus obtain

$$\|u - u_\ell\|_{H^1(\Omega)} \lesssim \|\tilde{u} - \tilde{u}_\ell\|_{H^1(\Omega)} + \|g - g_\ell\|_{H^{1/2}(\Gamma)} \xrightarrow{\ell \rightarrow \infty} 0$$

and conclude the proof. \square

5.2. Some elementary preliminaries. The next result is an elementary lemma for variational inequalities, see e.g. [33, Proposition 2].

Lemma 14. *Suppose that \mathcal{A} is a convex subset of $H^1(\Omega)$ and $f \in L^2(\Omega)$. Let $U \in \mathcal{A}$ be the solution of the variational inequality*

$$(37) \quad \langle U, V - U \rangle \geq (f, V - U) \quad \text{for all } V \in \mathcal{A}.$$

Then, for all $W \in \mathcal{A}$, there holds

$$(38) \quad \frac{1}{2} \|U - W\|^2 \leq \mathcal{J}(W) - \mathcal{J}(U),$$

i.e. the difference in the H^1 -seminorm is controlled in terms of the energy. □

5.3. Proof of Theorem 7. We start with estimate (25), where the lower estimate clearly holds due to Lemma 14. We thus only need to show the upper estimate. To that end, we define $\sigma_\ell \in H^{-1}(\Omega)$ by

$$\langle \sigma_\ell, v \rangle := (f, v) - \langle u_\ell, v \rangle \quad \text{for all } v \in H_0^1(\Omega).$$

Since $u_\ell|_\Gamma = U_\ell|_\Gamma$, we may argue as in the proof of [10, Theorem 1] to see

$$\|u_\ell - U_\ell\|^2 + \langle \sigma_\ell, u_\ell - U_\ell \rangle \lesssim \tilde{\varrho}_\ell^2,$$

where the hidden constant depends only on the shape regularity constant $\sigma(\mathcal{T}_\ell)$. A direct calculation finally shows

$$\begin{aligned} \mathcal{J}(U_\ell) - \mathcal{J}(u_\ell) &= \frac{1}{2} \langle U_\ell, U_\ell \rangle - (f, U_\ell) - \left(\frac{1}{2} \langle u_\ell, u_\ell \rangle - (f, u_\ell) \right) \\ &\quad + (\langle u_\ell, u_\ell - U_\ell \rangle - (f, u_\ell - U_\ell) + \langle \sigma_\ell, u_\ell - U_\ell \rangle) \\ &= \frac{1}{2} \|u_\ell - U_\ell\|^2 + \langle \sigma_\ell, u_\ell - U_\ell \rangle, \end{aligned}$$

whence $\mathcal{J}(U_\ell) - \mathcal{J}(u_\ell) \lesssim \tilde{\varrho}_\ell^2$.

Next we prove (27). According to the Rellich compactness theorem and the triangle inequality, there holds

$$\begin{aligned} \|u - U_\ell\|_{H^1(\Omega)} &\simeq \|u - U_\ell\| + \|g - g_\ell\|_{H^{1/2}(\Gamma)} \\ &\leq \|u - u_\ell\| + \|u_\ell - U_\ell\| + \|g - g_\ell\|_{H^{1/2}(\Gamma)}. \end{aligned}$$

From (25), we infer

$$\|u_\ell - U_\ell\|^2 \lesssim \tilde{\varrho}_\ell^2 \leq \varrho_\ell^2.$$

From [4, Lemma 2.2], we additionally infer that

$$\|g - g_\ell\|_{H^{1/2}(\Gamma)}^2 \lesssim \sum_{E \in \mathcal{E}_\ell^\Gamma} \text{apx}_\ell(E)^2 \leq \varrho_\ell^2,$$

and the constant depends only on Γ and the local mesh ratio of $\mathcal{E}_\ell^\Gamma = \mathcal{T}_\ell|_\Gamma$, whence on Ω and $\sigma(\mathcal{T}_\ell)$. The combination of the last three estimates yields (27). Moreover, according to the last estimate, the convergence $\varrho_\ell \rightarrow 0$ implies $g_\ell \rightarrow g$ in $H^{1/2}(\Gamma)$ as $\ell \rightarrow \infty$. According to the stability result from Proposition 13, this yields convergence $u_\ell \rightarrow u$ in $H^1(\Omega)$, and we also conclude the proof of (28). □

6. Proof of Theorem 10 (Convergence of AFEM)

The idea of our convergence proof is roughly sketched as follows: Dörfler marking (29) yields that ϱ_ℓ is contractive up to $\|U_{\ell+1} - U_\ell\|$, see Section 6.1. Since there seems to be no estimate for this term to be available (recall nonconformity $\mathcal{A}_\ell \not\subseteq \mathcal{A}_{\ell+1}$), we introduce a discrete auxiliary problem with solution $U_{\ell+1,\ell}$ which allows to control

$$\|U_{\ell+1} - U_\ell\| \leq \|U_{\ell+1} - U_{\ell+1,\ell}\| + \|U_{\ell+1,\ell} - U_\ell\|$$

in terms of the energy $\mathcal{J}(U_\ell) - \mathcal{J}(U_{\ell+1,\ell})$, see Section 6.3. In Section 6.4, we finally follow the concept of [16] to prove Theorem 10.

6.1. Estimator reduction. The following contraction estimate is called *estimator reduction* in [3, 16].

Proposition 15. *Suppose that the set $\mathcal{M}_\ell \subseteq \mathcal{E}_\ell$ satisfies (29) and that marked edges are refined as stated in Section 4.1. Then, there holds*

$$(39) \quad \varrho_{\ell+1}^2 \leq q \varrho_\ell^2 + C_4 \|U_{\ell+1} - U_\ell\|^2$$

with some contraction constant $q \in (0, 1)$ which depends only on $\theta \in (0, 1)$. The constant $C_4 > 0$ additionally depends only on the initial mesh \mathcal{T}_0 .

Since the proof of Proposition 15 follows along the lines of the proof of [33, Proposition 3], we only sketch it for brevity.

Sketch of proof. First, the Young inequality proves for arbitrary $\delta > 0$

$$(40) \quad \begin{aligned} \varrho_{\ell+1}^2 &\leq \sum_{E' \in \mathcal{E}_{\ell+1}} \text{osc}_{\ell+1}(E')^2 + \sum_{E' \in \mathcal{E}_{\ell+1}^\Gamma} \text{apx}_{\ell+1}(E')^2 \\ &\quad + (1 + \delta) \sum_{E' \in \mathcal{E}_{\ell+1}^\Omega} h_{E'} \|\partial_n U_\ell\|_{L^2(E')}^2 + (1 + \delta^{-1}) \sum_{E' \in \mathcal{E}_{\ell+1}^\Omega} h_{E'} \|\partial_n(U_{\ell+1} - U_\ell)\|_{L^2(E')}^2. \end{aligned}$$

A scaling argument allows to estimate the last term by

$$(41) \quad \sum_{E' \in \mathcal{E}_{\ell+1}^\Omega} h_{E'} \|\partial_n(U_{\ell+1} - U_\ell)\|_{L^2(E')}^2 \leq C \|U_{\ell+1} - U_\ell\|^2,$$

and the constant $C > 0$ depends only on $\sigma(\mathcal{T}_\ell)$. Next, one investigates the reduction of the other three terms if the mesh is refined locally: According to [33, Lemma 5], it holds that

$$(42) \quad \sum_{E' \in \mathcal{E}_{\ell+1}^\Omega} h_{E'} \|\partial_n U_\ell\|_{L^2(E')}^2 \leq \sum_{E \in \mathcal{E}_\ell^\Omega} \eta_\ell(E)^2 - \frac{1}{2} \sum_{E \in \mathcal{E}_\ell^\Omega \cap \mathcal{M}_\ell} \eta_\ell(E)^2.$$

Next, [33, Lemma 6] resp. [32, Lemma 3.9.6] yields

$$(43) \quad \sum_{E' \in \mathcal{E}_{\ell+1}} \text{osc}_{\ell+1}(E')^2 \leq \sum_{E \in \mathcal{E}_\ell} \text{osc}_\ell(E)^2 - \frac{1}{4} \sum_{E \in \mathcal{E}_\ell \cap \mathcal{M}_\ell} \text{osc}_\ell(E)^2.$$

Moreover, it is part of the proof of [2, Theorem 5.4] that

$$(44) \quad \sum_{E' \in \mathcal{E}_{\ell+1}^\Gamma} \text{apx}_{\ell+1}(E')^2 \leq \sum_{E \in \mathcal{E}_\ell^\Gamma} \text{apx}_\ell(E)^2 - \frac{1}{2} \sum_{E \in \mathcal{E}_\ell^\Gamma \cap \mathcal{M}_\ell} \text{apx}_\ell(E)^2.$$

Combining the estimates (40)–(44) and using the Dörfler marking (29), we easily obtain

$$\varrho_{\ell+1}^2 \leq (1 + \delta)(1 - \theta/4) \varrho_\ell^2 + (1 + \delta^{-1})C \|U_{\ell+1} - U_\ell\|^2.$$

Finally, we may choose $\delta > 0$ sufficiently small to guarantee $q := (1 + \delta)(1 - \theta/4) < 1$ to end up with (39). \square

Remark 16. *In the conforming case $\mathcal{A}_\ell \subseteq \mathcal{A}_{\ell+1}$, it is easily seen that the sequence U_ℓ of discrete solutions tends to some limit U_∞ which is the unique Galerkin solution with respect to the closure of $\bigcup_{\ell=0}^\infty \mathcal{A}_\ell$, see [32, Lemma 3.3.8]. Therefore, $\lim_\ell \|U_{\ell+1} - U_\ell\| = 0$, and elementary calculus predicts that (39) already implies $\lim_\ell \varrho_\ell = 0$, cf. e.g. [3, Proposition 1.2]. Then, Theorem 7 would conclude that $\lim_\ell \|u - U_\ell\|_{H^1(\Omega)} = 0$, i.e. $u = U_\infty$. — Now that $\mathcal{A}_\ell \not\subseteq \mathcal{A}_{\ell+1}$, we did neither succeed to prove that the a priori limit U_∞ exists nor the much weaker claim that $\lim_\ell \|U_{\ell+1} - U_\ell\| = 0$.*

6.2. Some a priori convergence results. In the adaptive algorithm, the mesh $\mathcal{T}_{\ell+1}$ is obtained by local refinement of elements in \mathcal{T}_ℓ , see Section 4.1. Consequently, the discrete spaces $\mathcal{S}^1(\mathcal{T}_\ell)$ are nested, i.e.,

$$(45) \quad \mathcal{S}^1(\mathcal{T}_\ell) \subseteq \mathcal{S}^1(\mathcal{T}_{\ell+1}) \quad \text{for all } \ell \in \mathbb{N}$$

and the analogous inclusion also holds for the spaces $\mathcal{S}^1(\mathcal{T}_\ell|_\Gamma) \subseteq \mathcal{S}^1(\mathcal{T}_{\ell+1}|_\Gamma)$ on the boundary. This is exploited in the following lemma which is part of the proof of [1, Proposition 10].

Lemma 17. *The nodal interpolants $g_\ell \in \mathcal{S}^1(\mathcal{T}_\ell|_\Gamma)$ of some Dirichlet data $g \in H^1(\Gamma)$ converge to some a priori limit in $H^1(\Gamma)$, i.e. there holds*

$$(46) \quad \|g_\infty - g_\ell\|_{H^1(\Gamma)} \xrightarrow{\ell \rightarrow \infty} 0$$

for a certain element $g_\infty \in H^1(\Gamma)$. \square

In the following, we will only use the convergence of g_ℓ to g_∞ in $H^{1/2}(\Gamma)$ as well as the uniform boundedness $\sup_{\ell \in \mathbb{N}} \|g_\ell\|_{H^{1/2}(\Gamma)} < \infty$ which is an immediate consequence.

Proposition 18. *The sequence $u_\ell \in \mathcal{A}_\ell^*$ of solutions of the continuous auxiliary problem (24) converges to some a priori limit $u_\infty \in H^1(\Omega)$, i.e.*

$$(47) \quad \|u_\infty - u_\ell\|_{H^1(\Omega)} \xrightarrow{\ell \rightarrow \infty} 0$$

for some function $u_\infty \in H^1(\Omega)$. In particular, there holds

$$(48) \quad \mathcal{J}(u_\infty) = \lim_{\ell \rightarrow \infty} \mathcal{J}(u_\ell).$$

Proof. Since convergence in $H^1(\Gamma)$ implies convergence in $L^2(\Gamma)$, the Weyl theorem applies and proves that a subsequence (g_{ℓ_k}) converges to g_∞ pointwise almost everywhere on Γ . Therefore, the limit function $g_\infty \in H^1(\Gamma)$ satisfies $g_\infty \geq \chi$ almost everywhere on Γ . In particular, the obstacle problem (13) with $g = g_\infty$ has also a unique solution $u_\infty \in H^1(\Gamma)$. Applying the stability result from Proposition 13, we obtain convergence of u_ℓ to u_∞ in $H^1(\Omega)$ as $\ell \rightarrow \infty$. \square

6.3. Discrete energy estimates. The main difficulty which we suffered in our analysis is that it is not clear that $\|U_{\ell+1} - U_\ell\|$ resp. $\mathcal{J}(U_{\ell+1}) - \mathcal{J}(U_\ell)$ tend

to zero as $\ell \rightarrow \infty$. We circumvent this question by introducing a discrete auxiliary problem: Find $U_{\ell+1,\ell} \in \mathcal{A}_{\ell+1,\ell}$ such that

$$(49a) \quad \mathcal{J}(U_{\ell+1,\ell}) = \min_{V_{\ell+1} \in \mathcal{A}_{\ell+1,\ell}} \mathcal{J}(V_{\ell+1}).$$

where the admissible set reads

$$(49b) \quad \mathcal{A}_{\ell+1,\ell} := \{V_{\ell+1} \in \mathcal{S}^1(\mathcal{T}_{\ell+1}) : V_{\ell+1} \geq \chi \text{ in } \Omega, V_{\ell+1} = g_\ell \text{ on } \Gamma\}.$$

Applying Proposition 6 to the data $(\mathcal{A}_{\ell+1,\ell}, g_\ell)$ instead of $(\mathcal{A}_\ell, g_\ell)$, we see that the auxiliary problem (49) admits a unique solution $U_{\ell+1,\ell} \in \mathcal{A}_{\ell+1,\ell}$.

Our first lemma is a key ingredient of the upcoming proofs. It states that one may change the boundary data of a discrete function and control the influence within Ω .

Lemma 19. *Let $W_{\ell+1} \in \mathcal{S}^1(\mathcal{T}_{\ell+1})$ with $W_{\ell+1}|_\Gamma = g_{\ell+1}$. Define $W_{\ell+1}^\ell \in \mathcal{S}^1(\mathcal{T}_{\ell+1})$ by*

$$(50) \quad W_{\ell+1}^\ell(z) = \begin{cases} W_{\ell+1}(z) & \text{for } z \in \mathcal{N}_{\ell+1} \setminus \Gamma, \\ g_\ell(z) & \text{for } z \in \mathcal{N}_{\ell+1} \cap \Gamma. \end{cases}$$

Then, with the local mesh-width $h_\ell \in L^\infty(\Gamma)$ defined by $h_\ell|_E = h_E$, there holds

$$(51) \quad \|W_{\ell+1} - W_{\ell+1}^\ell\|_{H^1(\Omega)} \leq C_5 \|h_\ell^{1/2}(g_{\ell+1} - g_\ell)'\|_{L^2(\Gamma)} \leq C_6 \|g_{\ell+1} - g_\ell\|_{H^{1/2}(\Gamma)},$$

where $C_5, C_6 > 0$ depend only on \mathcal{T}_0 and on Ω .

Proof. By definition, we have $W_{\ell+1}^\ell \in \mathcal{S}^1(\mathcal{T}_{\ell+1})$ with $W_{\ell+1}^\ell|_\Gamma = g_\ell$. Moreover, there holds $W_{\ell+1}^\ell|_T = W_{\ell+1}|_T$ for all $T \in \mathcal{T}_{\ell+1} \setminus \mathcal{T}_{\ell+1}^\Gamma$. Let $T = \text{conv}\{z_1, z_2, z_3\} \in \mathcal{T}_{\ell+1}^\Gamma$ and $\Phi_T : T_{\text{ref}} \rightarrow T$ be the affine diffeomorphism with reference element $T_{\text{ref}} = \text{conv}\{(0, 0), (0, 1), (1, 0)\}$.

The transformation formula and norm equivalence on $\mathcal{P}^1(T_{\text{ref}})$ prove

$$\begin{aligned} \|W_{\ell+1} - W_{\ell+1}^\ell\|_{L^2(T)} &= |T|^{1/2} \|(W_{\ell+1} - W_{\ell+1}^\ell) \circ \Phi_T\|_{L^2(T_{\text{ref}})} \\ &\lesssim |T|^{1/2} \sum_{j=1}^3 |(W_{\ell+1} - W_{\ell+1}^\ell) \circ \Phi_T(z_j^{\text{ref}})| \\ &\leq |\Omega|^{1/2} \sum_{j=1}^3 |(W_{\ell+1} - W_{\ell+1}^\ell)(z_j)| \end{aligned}$$

as well as

$$\begin{aligned} \|\nabla(W_{\ell+1} - W_{\ell+1}^\ell)\|_{L^2(T)} &\lesssim \sigma(\mathcal{T}_\ell) \|\nabla((W_{\ell+1} - W_{\ell+1}^\ell) \circ \Phi_T)\|_{L^2(T_{\text{ref}})} \\ &\lesssim \sigma(\mathcal{T}_\ell) \sum_{j=1}^3 |(W_{\ell+1} - W_{\ell+1}^\ell)(z_j)|. \end{aligned}$$

Now, we consider the nodes $z \in \{z_1, z_2, z_3\}$ of the triangle T : For $z \in \mathcal{N}_\ell \cap \Gamma$ holds $g_\ell(z) = g_{\ell+1}(z)$ by definition of the nodal interpolants. Therefore,

$$(W_{\ell+1} - W_{\ell+1}^\ell)(z) = 0 \quad \text{if } z \in (\mathcal{N}_{\ell+1} \cap \Omega) \cup (\mathcal{N}_\ell \cap \Gamma).$$

Thus, it only remains to consider nodes $z \in (\mathcal{N}_{\ell+1} \setminus \mathcal{N}_\ell) \cap \Gamma$. In this case (see Section 4.1), z is the midpoint of a refined edge \widehat{E}_z of the unique father $\widehat{T} \in \mathcal{T}_\ell$ with $T \subseteq \widehat{T}$, and there even holds $\widehat{E}_z \subset \Gamma$. Let $\widehat{z} \in \mathcal{N}_\ell$ be an arbitrary endpoint of \widehat{E}_z . Then,

$$(W_{\ell+1} - W_{\ell+1}^\ell)(\widehat{z}) = (g_{\ell+1} - g_\ell)(\widehat{z}) = 0,$$

and the fundamental theorem of calculus, now applied for the arclength derivative, yields

$$|(W_{\ell+1} - W_{\ell+1}^\ell)(z)| \leq \left| \int_{\hat{z}}^z (g_{\ell+1} - g_\ell)' d\Gamma \right| \leq |z - \hat{z}|^{1/2} \|(g_\ell - g_{\ell+1})'\|_{L^2(\hat{E}_z)}.$$

Combining our observations, we have now shown

$$\|W_{\ell+1} - W_{\ell+1}^\ell\|_{H^1(T)} \lesssim \sum_{\substack{\hat{E} \in \mathcal{E}_\ell^\Gamma \\ \hat{E} \subset \partial \hat{T}}} h_{\hat{E}}^{1/2} \|(g_\ell - g_{\ell+1})'\|_{L^2(\hat{E})} \simeq \left(\sum_{\substack{\hat{E} \in \mathcal{E}_\ell^\Gamma \\ \hat{E} \subset \partial \hat{T}}} h_{\hat{E}} \|(g_\ell - g_{\ell+1})'\|_{L^2(\hat{E})}^2 \right)^{1/2}.$$

Finally, note that each edge $\hat{E} \in \mathcal{E}_\ell^\Gamma$ belongs only to one element $\hat{T} \in \mathcal{T}_\ell$. Thus, \hat{E} can at most be selected by all (but at most four) sons $T \in \mathcal{T}_{\ell+1}$ of \hat{T} , cf. Figure 1. This observation yields

$$\|W_{\ell+1} - W_{\ell+1}^\ell\|_{H^1(\Omega)}^2 = \sum_{T \in \mathcal{T}_{\ell+1}^\Gamma} \|W_{\ell+1} - W_{\ell+1}^\ell\|_{H^1(T)}^2 \lesssim \sum_{\hat{E} \in \mathcal{E}_\ell^\Gamma} h_{\hat{E}}^{1/2} \|(g_\ell - g_{\ell+1})'\|_{L^2(\hat{E})}^2.$$

With the local mesh-width function $h_\ell \in L^\infty(\Gamma)$, this estimate reads

$$\|W_{\ell+1} - W_{\ell+1}^\ell\|_{H^1(\Omega)} \lesssim \|h_\ell^{1/2} (g_\ell - g_{\ell+1})'\|_{L^2(\Gamma)} \lesssim \|g_\ell - g_{\ell+1}\|_{H^{1/2}(\Gamma)},$$

where we have used a local inverse estimate from [15, Proposition 3.1] in the last step. We stress that the constant depends only on the local mesh-ratio of $\mathcal{T}_{\ell+1}|_\Gamma$, whence on $\sigma(\mathcal{T}_{\ell+1})$. This concludes the proof. \square

With the notation of Lemma 19, we can now formulate an additional convergence result.

Proposition 20. *The sequence of discrete solutions $U_{\ell+1,\ell} \in \mathcal{A}_{\ell+1,\ell}$ satisfies*

(52)

$$|\mathcal{J}(U_{\ell+1,\ell}) - \mathcal{J}(U_{\ell+1})| + |\mathcal{J}(U_{\ell+1,\ell}) - \mathcal{J}(U_{\ell+1}^\ell)| \leq C_7 \|g_{\ell+1} - g_\ell\|_{H^{1/2}(\Gamma)} \xrightarrow{\ell \rightarrow \infty} 0$$

with some constant $C_7 > 0$ which only depends on \mathcal{T}_0 .

To prove Proposition 20, we start with the observation that the energy functional $\mathcal{J}(\cdot)$ is coercive.

Lemma 21. *For each sequence $w_\ell \in H^1(\Omega)$ with changing boundary data $w_\ell|_\Gamma = g_\ell$, bounded energy implies uniform boundedness in $H^1(\Omega)$, i.e.*

$$(53) \quad \sup_{\ell \in \mathbb{N}} \mathcal{J}(w_\ell) < \infty \implies \sup_{\ell \in \mathbb{N}} \|w_\ell\|_{H^1(\Omega)} < \infty.$$

Proof. Note that triangle inequalities and the Friedrichs inequality yield

$$\begin{aligned} \|w_\ell\|_{L^2(\Omega)} &\leq \|w_\ell - \mathcal{L}g_\ell\|_{L^2(\Omega)} + \|\mathcal{L}g_\ell\|_{L^2(\Omega)} \\ &\lesssim \|\nabla(w_\ell - \mathcal{L}g_\ell)\|_{L^2(\Omega)} + \|\mathcal{L}g_\ell\|_{L^2(\Omega)} \\ &\lesssim \|\nabla w_\ell\|_{L^2(\Omega)} + \|\mathcal{L}g_\ell\|_{H^1(\Omega)} \\ &\lesssim \|\nabla w_\ell\|_{L^2(\Omega)} + M \end{aligned}$$

with $M = \sup_\ell \|g_\ell\|_{H^{1/2}(\Gamma)} < \infty$, where we have finally used continuity of \mathcal{L} and a priori convergence of g_ℓ , cf. Lemma 17. Consequently, we obtain

$$\|w_\ell\|_{H^1(\Omega)} \lesssim \|\nabla w_\ell\|_{L^2(\Omega)} + M$$

and therefore

$$\mathcal{J}(w_\ell) = \frac{1}{2} \|\nabla w_\ell\|_{L^2(\Omega)}^2 - (f, w_\ell) \gtrsim (\|w_\ell\|_{H^1(\Omega)} - M)^2 - \|f\|_{L^2(\Omega)} \|w_\ell\|_{H^1(\Omega)}.$$

The implication (53) is an immediate consequence. \square

Lemma 22. *The sequence of discrete solutions $U_\ell \in \mathcal{A}_\ell$ from Algorithm 9 satisfies*

$$(54) \quad \sup_{\ell \in \mathbb{N}} |\mathcal{J}(U_\ell)| < \infty \quad \text{as well as} \quad \sup_{\ell \in \mathbb{N}} \|U_\ell\|_{H^1(\Omega)} < \infty.$$

Proof. According to Lemma 21 with $w_\ell = U_\ell$, it is sufficient to prove boundedness of the energy. To that end, we define

$$V_\ell := \max_\ell \{P_\ell \mathcal{L}g_\ell - \chi, 0\} + \chi \in \mathcal{A}_\ell,$$

where \max_ℓ denotes the nodewise max-function, i.e. $\max_\ell \{v, w\} \in \mathcal{S}^1(\mathcal{T}_\ell)$ is defined by

$$\max_\ell \{v, w\}(z) := \max\{v(z), w(z)\} \quad \text{for all } z \in \mathcal{N}_\ell.$$

We consider the function $W_\ell := \max_\ell \{P_\ell \mathcal{L}g_\ell - \chi, 0\}$. Note that, by definition, $|W_\ell(z)| \leq |(P_\ell \mathcal{L}g_\ell - \chi)(z)|$ for all $z \in \mathcal{N}_\ell$. According to a standard scaling argument and $P_\ell \mathcal{L}g_\ell - \chi \in \mathcal{S}^1(\mathcal{T}_\ell)$, we infer, for all $T \in \mathcal{T}_\ell$,

$$\|W_\ell\|_{L^2(T)} \lesssim \|P_\ell \mathcal{L}g_\ell - \chi\|_{L^2(T)} \quad \text{as well as} \quad \|\nabla W_\ell\|_{L^2(T)} \lesssim \|\nabla(P_\ell \mathcal{L}g_\ell - \chi)\|_{L^2(T)}$$

due to the nodewise estimate. From this, we obtain a constant $C > 0$ with

$$\|V_\ell\|_{H^1(\Omega)} \lesssim \|P_\ell \mathcal{L}g_\ell - \chi\|_{H^1(\Omega)} + \|\chi\|_{H^1(\Omega)} \lesssim \|g_\ell\|_{H^{1/2}(\Gamma)} + \|\chi\|_{H^1(\Omega)} \leq C < \infty$$

since $\sup_\ell \|g_\ell\|_{H^{1/2}(\Gamma)} < \infty$ and the operator norm of P_ℓ depends only on $\sigma(\mathcal{T}_\ell)$. Therefore,

$$\mathcal{J}(U_\ell) \leq \mathcal{J}(V_\ell) = \frac{1}{2} \|\nabla V_\ell\|_{L^2(\Omega)}^2 - (f, V_\ell) \lesssim C(C + \|f\|_{L^2(\Omega)}) < \infty$$

yields $\sup_{\ell \in \mathbb{N}} \mathcal{J}(U_\ell) < \infty$ and concludes the proof. \square

Proof of Proposition 20. According to Lemma 22, we have $M := \sup_\ell \|U_\ell\|_{H^1(\Omega)} < \infty$. With the aid of Lemma 19, we obtain

$$(55) \quad \begin{aligned} \mathcal{J}(U_{\ell+1,\ell}) &\leq \mathcal{J}(U_{\ell+1}^\ell) = \frac{1}{2} \|U_{\ell+1}^\ell\|^2 - (f, U_{\ell+1}^\ell) \\ &\leq \frac{1}{2} (\|U_{\ell+1}\| + \|U_{\ell+1}^\ell - U_{\ell+1}\|)^2 - (f, U_{\ell+1}) + \|f\|_{L^2(\Omega)} \|U_{\ell+1}^\ell - U_{\ell+1}\|_{L^2(\Omega)} \\ &= \mathcal{J}(U_{\ell+1}) + \frac{1}{2} \|U_{\ell+1}^\ell - U_{\ell+1}\|^2 + \|U_{\ell+1}\| \|U_{\ell+1}^\ell - U_{\ell+1}\| + \|f\|_{L^2(\Omega)} \|U_{\ell+1}^\ell - U_{\ell+1}\|_{L^2(\Omega)} \\ &\leq \mathcal{J}(U_{\ell+1}) + \frac{1}{2} C_6^2 \|g_\ell - g_{\ell+1}\|_{H^{1/2}(\Gamma)}^2 + C_6 (M + \|f\|_{L^2(\Omega)}) \|g_{\ell+1} - g_\ell\|_{H^{1/2}(\Gamma)}, \end{aligned}$$

whence

$$\mathcal{J}(U_{\ell+1,\ell}) - \mathcal{J}(U_{\ell+1}) \lesssim \|g_\ell - g_{\ell+1}\|_{H^{1/2}(\Gamma)}^2 + \|g_{\ell+1} - g_\ell\|_{H^{1/2}(\Gamma)}.$$

Estimate (55) now reveals $\sup_\ell \mathcal{J}(U_{\ell+1,\ell}) < \infty$, whence $\sup_\ell \|U_{\ell+1,\ell}\|_{H^1(\Omega)} < \infty$ according to Lemma 21 with $w_\ell = U_{\ell+1,\ell}$. Arguing as in (55) with the ansatz $\mathcal{J}(U_{\ell+1}) \leq \mathcal{J}(U_{\ell+1,\ell}^{\ell+1})$ shows

$$\mathcal{J}(U_{\ell+1}) - \mathcal{J}(U_{\ell+1,\ell}) \lesssim \|g_\ell - g_{\ell+1}\|_{H^{1/2}(\Gamma)}^2 + \|g_{\ell+1} - g_\ell\|_{H^{1/2}(\Gamma)}.$$

The combination of the last two inequalities yields

$$|\mathcal{J}(U_{\ell+1}) - \mathcal{J}(U_{\ell+1,\ell})| \lesssim \|g_\ell - g_{\ell+1}\|_{H^{1/2}(\Gamma)}^2 + \|g_{\ell+1} - g_\ell\|_{H^{1/2}(\Gamma)} \xrightarrow{\ell \rightarrow \infty} 0.$$

Finally, we recall $\mathcal{J}(U_{\ell+1,\ell}) \leq \mathcal{J}(U_{\ell+1}^\ell)$. Then, the above calculation also yields

$$\begin{aligned} |\mathcal{J}(U_{\ell+1}^\ell) - \mathcal{J}(U_{\ell+1,\ell})| &= \mathcal{J}(U_{\ell+1}^\ell) - \mathcal{J}(U_{\ell+1,\ell}) \\ &= [\mathcal{J}(U_{\ell+1}^\ell) - \mathcal{J}(U_{\ell+1})] + [\mathcal{J}(U_{\ell+1}) - \mathcal{J}(U_{\ell+1,\ell})] \\ &\lesssim \|g_\ell - g_{\ell+1}\|_{H^{1/2}(\Gamma)}^2 + \|g_{\ell+1} - g_\ell\|_{H^{1/2}(\Gamma)} \xrightarrow{\ell \rightarrow \infty} 0. \end{aligned}$$

This concludes the proof. \square

We are now ready to prove that the sequence $U_\ell \in \mathcal{A}_\ell$ of discrete solutions generated by Algorithm 9 indeed converges towards the exact solution $u \in \mathcal{A}$.

6.4. Proof of Theorem 10. With the help of Lemma 19 and Lemma 14 applied twice for $U_\ell \in \mathcal{A}_{\ell+1,\ell}$, and $U_{\ell+1}^\ell \in \mathcal{A}_{\ell+1,\ell}$, we obtain

$$\begin{aligned} \frac{1}{2} \|U_{\ell+1} - U_\ell\|^2 &\leq \|U_{\ell+1} - U_{\ell+1,\ell}\|^2 + \|U_{\ell+1,\ell} - U_\ell\|^2 \\ &\leq 2 \|U_{\ell+1} - U_{\ell+1}^\ell\|^2 + 2 \|U_{\ell+1}^\ell - U_{\ell+1,\ell}\|^2 + 2 [\mathcal{J}(U_\ell) - \mathcal{J}(U_{\ell+1,\ell})] \\ &\leq 2 C_5^2 \|h_\ell^{1/2}(g_{\ell+1} - g_\ell)'\|_{L^2(\Gamma)}^2 + 4 [\mathcal{J}(U_{\ell+1}^\ell) - \mathcal{J}(U_{\ell+1,\ell})] \\ &\quad + 2 [\mathcal{J}(U_\ell) - \mathcal{J}(U_{\ell+1,\ell})]. \end{aligned}$$

Recall that $\Delta_{\ell+1} = [\mathcal{J}(U_{\ell+1}) - \mathcal{J}(u_{\ell+1})] + \gamma \varrho_{\ell+1}^2 + \lambda \text{apx}_{\ell+1}^2$. We now use the last estimate to see

$$\begin{aligned} [\mathcal{J}(U_{\ell+1}) - \mathcal{J}(u_{\ell+1})] &= [\mathcal{J}(U_\ell) - \mathcal{J}(u_\ell)] + [\mathcal{J}(u_\ell) - \mathcal{J}(u_{\ell+1})] \\ &\quad + [\mathcal{J}(U_{\ell+1}) - \mathcal{J}(U_{\ell+1,\ell})] + [\mathcal{J}(U_{\ell+1,\ell}) - \mathcal{J}(U_\ell)] \\ &\leq [\mathcal{J}(U_\ell) - \mathcal{J}(u_\ell)] + [\mathcal{J}(u_\ell) - \mathcal{J}(u_{\ell+1})] \\ &\quad + [\mathcal{J}(U_{\ell+1}) - \mathcal{J}(U_{\ell+1,\ell})] + C_5^2 \|h_\ell^{1/2}(g_{\ell+1} - g_\ell)'\|_{L^2(\Gamma)}^2 \\ &\quad - \frac{1}{4} \|U_{\ell+1} - U_\ell\|^2 + 2 [\mathcal{J}(U_{\ell+1}^\ell) - \mathcal{J}(U_{\ell+1,\ell})]. \end{aligned}$$

Note that according to Proposition 18 and Proposition 20 it holds that

$$\alpha_\ell := |\mathcal{J}(u_\ell) - \mathcal{J}(u_{\ell+1})| + |\mathcal{J}(U_{\ell+1}) - \mathcal{J}(U_{\ell+1,\ell})| + 2 |\mathcal{J}(U_{\ell+1}^\ell) - \mathcal{J}(U_{\ell+1,\ell})|$$

tends to zero as $\ell \rightarrow \infty$. Next, we recall that on the 1D manifold Γ , the derivative g'_ℓ of the nodal interpolant is the elementwise best approximation of the derivative g' by piecewise constants, i.e.

$$(56) \quad \|h_\ell^{1/2}(g - g_{\ell+1})'\|_{L^2(\Gamma)}^2 + \|h_\ell^{1/2}(g_{\ell+1} - g_\ell)'\|_{L^2(\Gamma)}^2 = \|h_\ell^{1/2}(g - g_\ell)'\|_{L^2(\Gamma)}^2$$

according to the elementwise Pythagoras theorem. So far and with $\lambda = C_5^2$, we thus have derived

$$\begin{aligned} \Delta_{\ell+1} &\leq [\mathcal{J}(U_\ell) - \mathcal{J}(u_\ell)] + \gamma \varrho_{\ell+1}^2 + \lambda \text{apx}_{\ell+1}^2 + \lambda \|h_\ell^{1/2}(g_{\ell+1} - g_\ell)'\|_{L^2(\Gamma)}^2 \\ &\quad - \frac{1}{4} \|U_{\ell+1} - U_\ell\|^2 + \alpha_\ell, \\ &\leq [\mathcal{J}(U_\ell) - \mathcal{J}(u_\ell)] + \gamma \varrho_{\ell+1}^2 + \lambda \text{apx}_\ell^2 - \frac{1}{4} \|U_{\ell+1} - U_\ell\|^2 + \alpha_\ell, \end{aligned}$$

where we have used the Pythagoras theorem in the second step.

Next, the estimator reduction of Proposition 15 applies and provides constants $0 < q < 1$ and $C_4 > 0$ with

$$\begin{aligned} \Delta_{\ell+1} &\leq [\mathcal{J}(U_\ell) - \mathcal{J}(u_\ell)] + \gamma q \varrho_\ell^2 + \lambda \text{apx}_\ell^2 + \left(\gamma C_4 - \frac{1}{4}\right) \|U_{\ell+1} - U_\ell\|^2 + \alpha_\ell \\ &\leq [\mathcal{J}(U_\ell) - \mathcal{J}(u_\ell)] + \gamma q \varrho_\ell^2 + \lambda \text{apx}_\ell^2 + \alpha_\ell \end{aligned}$$

provided the constant $0 < \gamma < 1$ is chosen sufficiently small.

Next, from Theorem 7, we infer $C_3^{-2} [\mathcal{J}(U_\ell) - \mathcal{J}(u_\ell)] \leq \varrho_\ell^2$.

We plug this estimate into the last one and use the fact that $\text{apx}_\ell^2 \leq \varrho_\ell^2$ to see

$$\begin{aligned} \Delta_{\ell+1} &\leq (1 - \gamma \varepsilon C_3^{-2}) [\mathcal{J}(U_\ell) - \mathcal{J}(u_\ell)] + \gamma(q + 2\varepsilon) \varrho_\ell^2 + (1 - \varepsilon \gamma) \lambda \text{apx}_\ell^2 + \alpha_\ell \\ &\leq \kappa \Delta_\ell + \alpha_\ell, \end{aligned}$$

with $\kappa := \max\{1 - \gamma \varepsilon C_3^{-2}, q + 2\varepsilon, 1 - \gamma \varepsilon\}$. For $0 < 2\varepsilon < 1 - q$, we obtain $0 < \kappa < 1$ and conclude the proof of the contraction property (31).

The application of Lemma 14 for $\mathcal{A}_\ell \subseteq \mathcal{A}_\ell^*$ yields $\mathcal{J}(u_\ell) \leq \mathcal{J}(U_\ell)$ and hence $\Delta_\ell \geq 0$. Together with $\alpha_\ell \geq 0$ and $\alpha_\ell \rightarrow 0$, elementary calculus yields $\Delta_\ell \rightarrow 0$ as $\ell \rightarrow \infty$, cf. [3, Proposition 1.2]. From $0 \leq \varrho_\ell \lesssim \Delta_\ell$, we obtain $\lim_\ell \varrho_\ell = 0$, and the weak reliability of ϱ_ℓ stated in Theorem 7 concludes the proof of (32). \square

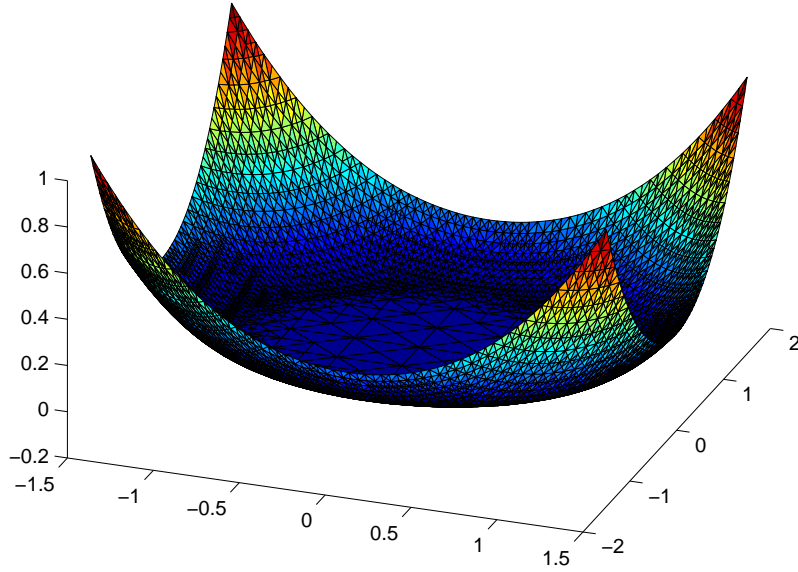


FIGURE 2. Galerkin solution U_6 on adaptively generated mesh \mathcal{T}_6 with $N = 4.159$ elements for $\theta = 0.8$.

7. Numerical Experiments

We consider numerical examples, one of which has also been treated in [10]. The mesh in each step is adaptively generated by Algorithm 9. For the solution at each level, we use the primal-dual active set strategy from [23]. The numerical results for example 1 are quite similar to those in [10]. We stress, however, that

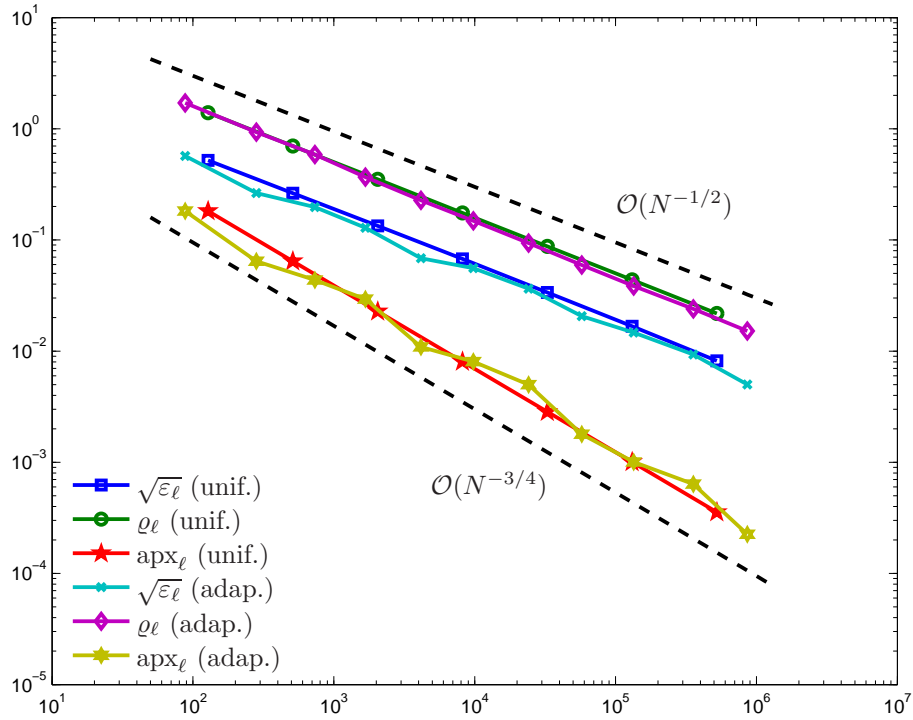


FIGURE 3. Numerical results for uniform and adaptive mesh-refinement with $\theta = 0.8$, where $\sqrt{\varepsilon_\ell}$, ϱ_ℓ , and apx_ℓ are plotted over the number of elements $N = \#\mathcal{T}_\ell$.

our approach includes the adaptive resolution of the Dirichlet data and, contrary to [10], the upcoming examples are thus covered by theory.

7.1. Example 1. We consider the obstacle problem with constant obstacle $\chi \equiv 0$ on the square $\Omega := (-1.5, 1.5)^2$ and a constant force $f \equiv -2$. The Dirichlet boundary data $g \in H^1(\Gamma)$ are given by the trace of the exact solution

$$u := \begin{cases} \frac{r^2}{2} - \ln(r) - \frac{1}{2}, & r \geq 1 \\ 0, & \text{else,} \end{cases}$$

where $r = |x|$ and $|\cdot|$ denotes the Euclidean norm on \mathbb{R}^2 . The solution is visualized in Figure 2. We compare uniform and adaptive mesh-refinement, where the adaptivity parameter θ varies between 0.4 and 0.8. The convergence history for uniform and adaptive refinement with $\theta = 0.8$ is plotted in Figure 3, where the error is given in the energy functional, i.e.

$$(57) \quad \varepsilon_\ell = |\mathcal{J}(U_\ell) - \mathcal{J}(u)|$$

and the Dirichlet data oscillations apx_ℓ are defined by (23). Note that due to Theorem 10, the adaptive algorithm drives the error and thus also the energy ε_ℓ to zero, whence it makes sense to plot these physically relevant terms. All quantities are plotted over the number of elements $N = \#\mathcal{T}_\ell$ of the given triangulation. Due to high regularity of the exact solution, there are no significant benefits of adaptive refinement. We observe, however, that error and error estimator, as well as Dirichlet oscillations show optimal convergence behaviour $\mathcal{O}(N^{-1/2})$ and $\mathcal{O}(N^{-3/4})$

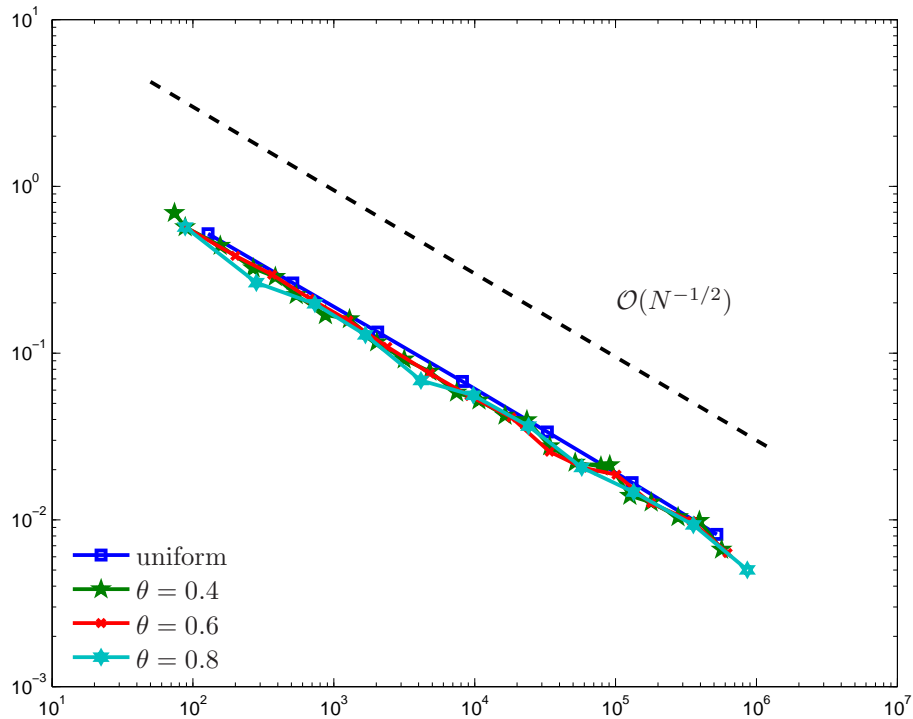


FIGURE 4. Numerical results for $\sqrt{\varepsilon_\ell}$ for uniform and adaptive mesh-refinement with $\theta \in \{0.4, 0.6, 0.8\}$, plotted over the number of elements $N = \#\mathcal{T}_\ell$.

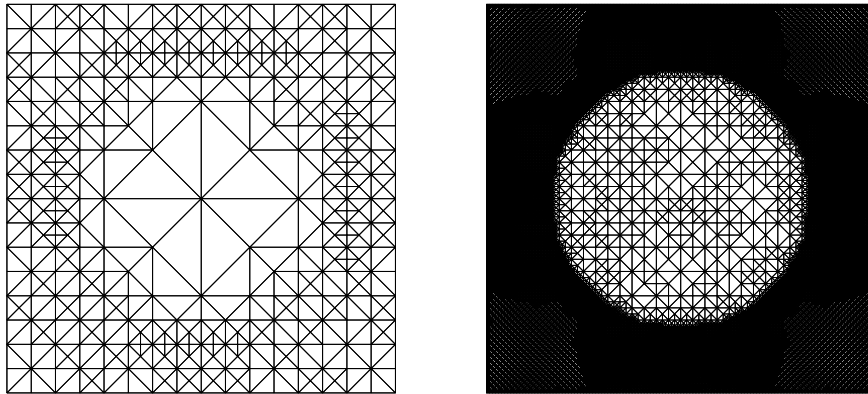


FIGURE 5. Adaptively generated meshes \mathcal{T}_5 (left) and \mathcal{T}_{11} (right) with $N = 678$ and $N = 34.024$ elements, respectively, for $\theta = 0.6$.

respectively. Also, the curves of ϱ_ℓ and $\sqrt{\varepsilon_\ell}$ are parallel, which experimentally confirms classical reliability and efficiency of the underlying estimator ϱ_ℓ in the sense of $\|u - U_\ell\|_{H^1(\Omega)} \simeq \varrho_\ell$.

Figure 4 compares different values of θ and we can see that each choice of $\theta \in \{0.4, 0.6, 0.8\}$ leads to optimal convergence, i.e. the curves basically coincide.

Finally, Figure 5 shows the adaptively generated meshes after 5 and 11 iterations. As expected, refinement basically takes place in the inactive zone, i.e. elements where the discrete solution U_ℓ does not touch the obstacle.

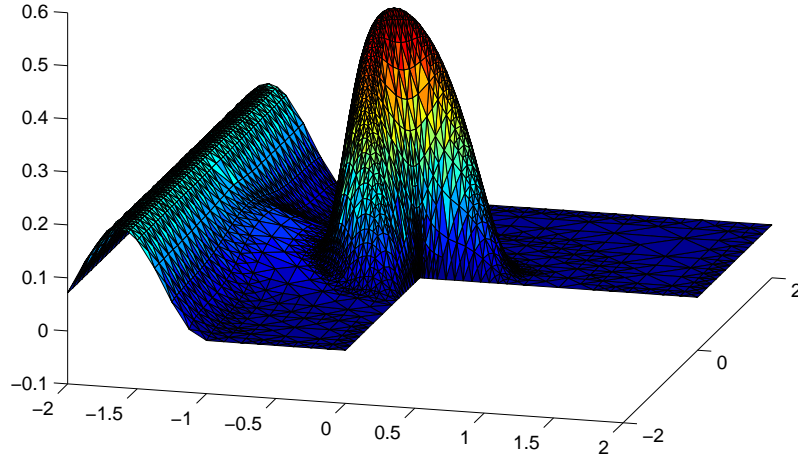


FIGURE 6. Galerkin solution U_{10} on adaptively generated mesh \mathcal{T}_{10} with $N = 8.870$ elements for $\theta = 0.6$.

7.2. Example 2. In this example, we consider the obstacle problem for a non-affine $H^2(\Omega)$ obstacle

$$\chi := \begin{cases} \frac{1}{10} [\sin(5(x + (1 - \pi/10))) + 1] & x < -1, \\ 0 & \text{else.} \end{cases}$$

on the L-shaped domain $\Omega := (-2, 2)^2 \setminus [-2, 0]$. The right hand side is given in polar coordinates by

$$f(r, \varphi) := -r^{2/3} \sin(2\varphi/3) (d/dr(\gamma_1)(r)/r + d^2/dr^2 \gamma_1(r)) - \frac{4}{3} r^{-1/3} d/dr(\gamma_1)(r) \sin(2\varphi/3) - \gamma_2(r),$$

where d/dr denotes the radial derivative. Moreover, $\bar{r} := 2(r - 1/4)$ and

$$\gamma_1(r) := \begin{cases} 1, & \bar{r} < 0, \\ -6\bar{r}^5 + 15\bar{r}^4 - 10\bar{r}^3 + 1, & 0 \leq \bar{r} < 1, \\ 0, & \bar{r} \geq 1, \end{cases}$$

$$\gamma_2(r) := \begin{cases} 0, & r \leq 5/4, \\ 1, & \text{else.} \end{cases}$$

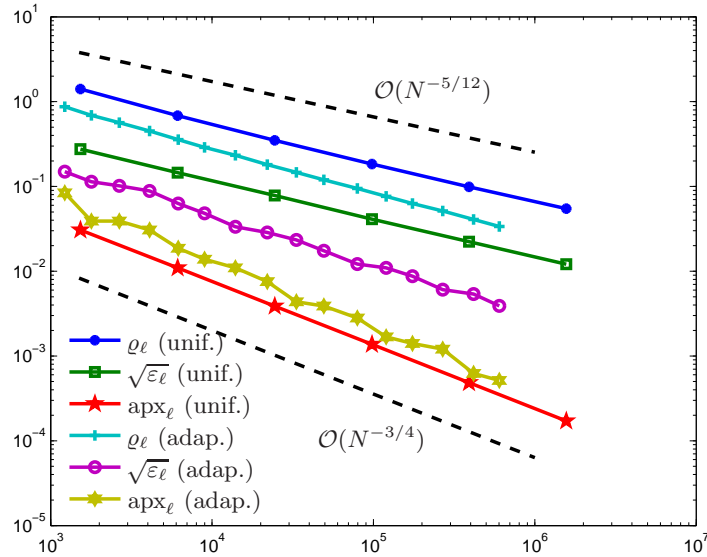


FIGURE 7. Numerical results for uniform and adaptive mesh-refinement with $\theta = 0.4$, where $\sqrt{\varepsilon_\ell}$, ρ_ℓ , and apx_ℓ are plotted over the number of elements $N = \#\mathcal{T}_\ell$.

The Dirichlet data $g \in H^{1/2}(\Gamma)$ are given by the trace of the obstacle χ . Since the exact solution for this problem is unknown, the Galerkin solution on a uniform mesh with approximately $N = \#\mathcal{T}_\ell = 1.500.000$ elements has been used as reference solution. The non-affine obstacle was treated by means of Proposition 4. Again, we compare uniform and adaptive mesh-refinement for different adaptivity parameters θ between 0.4 and 0.8. Figure 7 shows the convergence history for $\theta = 0.4$ plotted over the number of elements $N = \#\mathcal{T}_\ell$. As before, adaptive refinement leads to the optimal convergence rates $\mathcal{O}(N^{-1/2})$ and $\mathcal{O}(N^{-3/4})$ for $\sqrt{\varepsilon_\ell}$ and apx_ℓ , respectively. Due to the corner singularity of the exact solution at 0, we observe that uniform mesh-refinement leads to a suboptimal convergence behaviour.

Figure 8 compares the error for uniform and adaptive mesh refinement, where the adaptivity parameter θ varies between 0.4 and 0.8. Again, we observe that each adaptive strategy leads to optimal convergence rates, whereas the convergence rate for uniform refinement is suboptimal.

In Figure 9, the adaptively generated meshes after 13 and 18 iterations are visualized. As before, refinement is basically restricted to the inactive zone.

Acknowledgments

The authors M.F. and D.P. are funded by the Austria Science Fund (FWF) under grant P21732 *Adaptive Boundary Element Method*, which is thankfully acknowledged. M.P. acknowledges support through the project *Micromagnetic Simulations and Computational Design of Future Devices*, funded by the Viennese Science and Technology Fund (WWTF) under grant MA09-029.

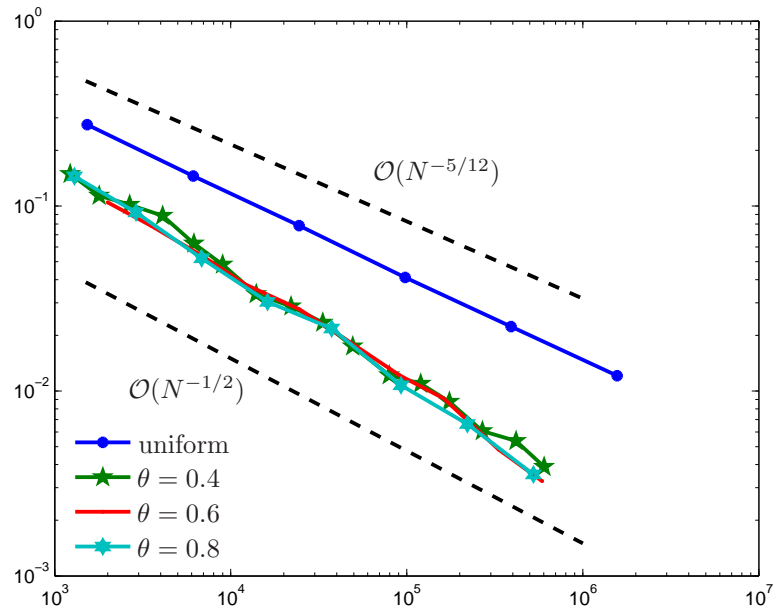


FIGURE 8. Numerical results for $\sqrt{\varepsilon_\ell}$ for uniform and adaptive mesh-refinement with $\theta \in \{0.4, 0.6, 0.8\}$, plotted over the number of elements $N = \#\mathcal{T}_\ell$.

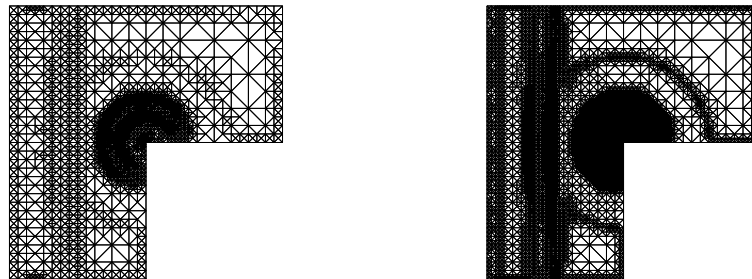


FIGURE 9. Adaptively generated meshes \mathcal{T}_{13} (left) and \mathcal{T}_{18} (right) with $N = 4.104$ and $N = 33.310$ elements, respectively, for $\theta = 0.6$.

References

- [1] M. AURADA, M. FEISCHL, D. PRAETORIUS: *Convergence of some adaptive FEM-BEM coupling for elliptic but possibly nonlinear interface problems*, M2AN Math. Model. Numer. Anal. **46** (2012), 1147–1173
- [2] M. AURADA, S. FERRAZ-LEITE, P. GOLDENITS, M. KARKULIK, M. MAYR, D. PRAETORIUS: *Convergence of adaptive BEM for some mixed boundary value problem*, Appl. Numer. Math. **62** (2012), 226–245.
- [3] M. AURADA, S. FERRAZ-LEITE, D. PRAETORIUS: *Estimator reduction and convergence of adaptive BEM*, Appl. Numer. Math. **62** (2012), 787–801.

- [4] C. ERATH, S. FUNKEN, P. GOLDENITS, D. PRAETORIUS: *Simple error estimators for the Galerkin BEM for some hypersingular integral equation in 2D*, Appl. Anal. **92** (2013), 1194–1216.
- [5] M. AINSWORTH, T. ODEN: *A posteriori error estimation in finite element analysis*, Wiley-Interscience, New-York, 2000.
- [6] M. AINSWORTH, C. LEE, T. ODEN: *Local a posteriori error estimators for variational inequalities*, Numer. Meth. Part. D. E. **9** (1993), 23–33.
- [7] D. BRAESS: *Finite Elemente*, Springer, Berlin-Heidelberg ⁴2007.
- [8] D. BRAESS: *A posteriori error estimators for obstacle problems — another look*, Numer. Math. **101** (2005), 415–421.
- [9] S. BARTELS, C. CARSTENSEN: *Averaging techniques yield reliable a posteriori finite element error control for obstacle problems*, Numer. Math. **99** (2004), 225–249.
- [10] D. BRAESS, C. CARSTENSEN, R. HOPPE: *Convergence analysis of a conforming adaptive finite element method for an obstacle problem*, Numer. Math. **107** (2007), 455–471.
- [11] D. BRAESS, C. CARSTENSEN, R. HOPPE: *Error reduction in adaptive finite element approximations of elliptic obstacle problems*, J. Comput. Math. **27** (2009), 148–169.
- [12] R. BECKER, S. MAO: *Convergence and quasi-optimal complexity of a simple adaptive finite element method*, M2AN Math. Model. Numer. Anal. **43** (2009), 1203–1219.
- [13] C. CARSTENSEN, R. HOPPE: *Error reduction and convergence for an adaptive mixed finite element method*, Math. Comp. **75** (2006), 1033–1042.
- [14] C. CARSTENSEN, R. HOPPE: *Convergence analysis of an adaptive nonconforming finite element method*, Numer. Math. **103** (2006), 251–266.
- [15] C. CARSTENSEN, D. PRAETORIUS: *Averaging techniques for the a posteriori BEM error control for a hypersingular integral equation in two dimensions*, SIAM J. Sci. Comput. **29** (2007), 782–810.
- [16] J. CASCON, C. KREUZER, R. NOCHETTO, K. SIEBERT: *Quasi-optimal convergence rate for an adaptive finite element method*, SIAM J. Numer. Anal. **46** (2008), 2524–2550.
- [17] Z. CHEN, R. NOCHETTO: *Residual type a posteriori error estimates for elliptic obstacle problems*, Numer. Math. **84** (2000), 527–548.
- [18] V. DOMINGUEZ, F. SAYAS: *Stability of discrete liftings*, C. R. Acad. Sci. Paris, Ser. I **337** (2003), 805–808.
- [19] W. DÖRFLER: *A convergent adaptive algorithm for Poisson’s equation*, SIAM J. Numer. Anal. **33** (1996), 1106–1124.
- [20] M. FEISCHL, M. PAGE, D. PRAETORIUS: *Convergence and quasi-optimality of adaptive FEM for the Poisson problem with inhomogeneous Dirichlet data*, J. Comput. Appl. Math. **255** (2014), 481–501.
- [21] A. FRIEDMANN: *Variational principles and free-boundary problems*, Wiley, New York 1982.
- [22] R. GLOWINSKI: *Numerical methods for nonlinear variational problems*, Springer, Berlin-Heidelberg 2008.
- [23] K. ITO, K. KUNISCH: *Lagrange multiplier approach to variational problems and applications*, SIAM, Advances in Design and Control, Philadelphia 2008.
- [24] M. KARKULIK, G. OF, D. PRAETORIUS: *Convergence of adaptive 3D BEM for weakly singular integral equations based on isotropic mesh-refinement*, Numer. Methods Partial Differential Equations **29** (2013), 2081–2106.
- [25] D. KINDERLEHRER, G. STAMPACCHIA: *An introduction to variational inequalities*, Academic Press, New York, 1980.
- [26] W. LIU, N. YAN: *A posteriori error estimates for a class of variational inequalities*, J. Sci. Comput. **15** (2000), 361–393.
- [27] W. MCLEAN: *Strongly elliptic systems and boundary integral equations*, Cambridge University Press, Cambridge 2000.
- [28] U. MOSCO: *Convergence of convex sets and of solutions of variational inequalities*, Advances in Math. **3** (1969), 510–585.
- [29] P. MORIN, R. NOCHETTO, K. SIEBERT: *Data oscillation and convergence of adaptive FEM*, SIAM. J. Numer. Anal. **18** (2000), 466–488.
- [30] P. MORIN, K. SIEBERT, A. VEESER: *A basic convergence result for conforming adaptive finite elements*, Math. Models Methods Appl. Sci. **18** (2008), 707–737.
- [31] R. NOCHETTO, K. SIEBERT, A. VEESER: *Fully localized a posteriori error estimators and barrier sets for contact problems*, SIAM J. Numer. Anal. **42** (2005), 2118–2135.

- [32] M. PAGE: *Schätzerreduktion und Konvergenz adaptiver FEM für Hindernisprobleme*, Master thesis (in German), Institute for Analysis and Scientific Computing, Vienna University of Technology, Wien 2010.
- [33] M. PAGE, D. PRAETORIUS: *Convergence of adaptive FEM for some elliptic obstacle problem*, Appl. Anal. **92** (2013), 595–615.
- [34] A. PETROSYAN, H. SHAHGHOLIAN: *Parabolic obstacle problems applied to finance*, Contemp. Math. **439**, Amer. Math. Society, Providence, RI, 2007.
- [35] J. RODRIGUES: *Obstacle problems in mathematical physics*, Elsevier Science Publishers B.V., Amsterdam 1987.
- [36] L. R. SCOTT, S. ZHANG: *Finite element interpolation of nonsmooth functions satisfying boundary conditions*, Math. Comp. **54** (1990), 483–493.
- [37] R. STEVENSON: *Optimality of standard adaptive finite element method*, Found. Comput. Math. (2007), 245–269.
- [38] R. VERFÜRTH: *A review of a posteriori error estimation and adaptive mesh-refinement techniques*, Wiley-Teubner, New York 1996.
- [39] A. VEESER: *Efficient and reliable a posteriori error estimators for elliptic obstacle problems*, SIAM J. Numer. Anal. **39** (2001), 146–167.
- [40] A. VEESER: *Convergent adaptive finite elements for the nonlinear Laplacian*, Numer. Math. **92** (2002), 743–770.

Institute for Analysis and Scientific Computing, Vienna University of Technology, Wiedner Hauptstraße 8-10, A-1040 Wien, Austria

E-mail: Michael.Feischl@tuwien.ac.at

E-mail: Marcus.Page@tuwien.ac.at

E-mail: Dirk.Praetorius@tuwien.ac.at